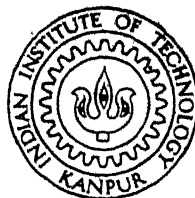


A STUDY OF THE INTERACTION OF A JET WITH A FREE SURFACE FLOW

by

MAHAVEER PRASAD JAIN



TH
CE/1970/M
J1998

DEPARTMENT OF CIVIL ENGINEERING
INDIAN INSTITUTE OF TECHNOLOGY KANPUR

NOVEMBER 1970

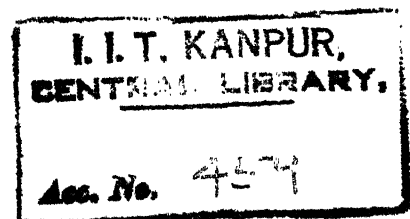
CE
1970
M
JAI
STU

A STUDY OF THE INTERACTION OF A JET
WITH A FREE SURFACE FLOW



A Thesis Submitted
In Partial Fulfilment of the Requirement
For the Degree of

MASTER OF TECHNOLOGY

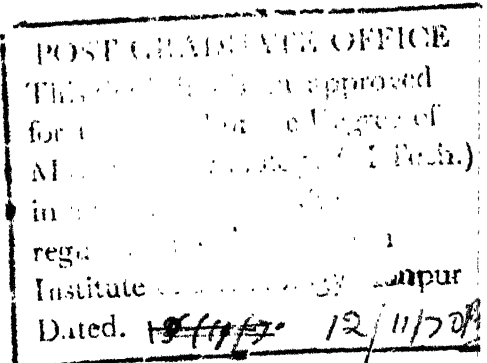


by

Mahaveer Prasad Jain

to the

Department of Civil Engineering
Indian Institute of Technology Kanpur



November 1970

CE-1970-M-JAI-DNT

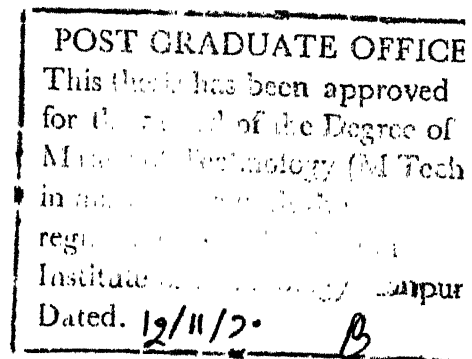
ACKNOWLEDGEMENTS

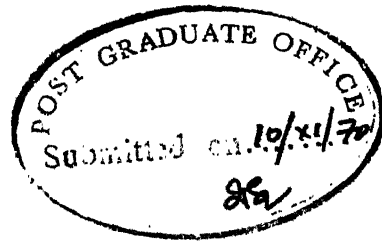
The author wishes to express his sincere thanks and gratitude to Dr. K. Subramanya, Assistant Professor, Department of Civil Engineering, for his encouraging guidance.

Thanks are also due to Mr. Suresh Kumar of the Hydraulics Laboratory and other staff members.

Finally, thanks are due to Mr. B.P. Shrestha and Mr. D.S. Notra who helped me in bringing up this thesis.

MAHAVEER PRASAD JAIN





CERTIFICATE

This is to certify that the thesis entitled
"A study of the interaction of a jet with a free surface
flow" by Shri M.P. Jain is record of work carried out
under my supervision and has not been submitted else-
where for a degree.

K. Subramanya.

(K Subramanya)
Assistant Professor
Civil Engineering Department
Indian Institute of Technology
Kanpur

CONTENTS

	Page
LIST OF FIGURES	i
NOTATIONS	iii
ABSTRACT	v
CHAPTER I INTRODUCTION	1
CHAPTER II EXPERIMENTAL SET-UP	7
CHAPTER III SUPER-CRITICAL FLOW INTERACTING WITH VERTICAL JET	13
CHAPTER IV SUB-CRITICAL FLOW INTERACTING WITH VERTICAL JET	36
CHAPTER V CONCLUSIONS	47
REFERENCES	
APPENDIX A EXPERIMENTAL DATA FOR SUPER- CRITICAL FLOW INTERACTING WITH VERTICAL JET	A-1
APPENDIX B EXPERIMENTAL DATA FOR TYPE B-JUMP	B-1
APPENDIX C DATA FOR TYPE B-JUMP (COMPUTED PARAMETERS)	C-1
APPENDIX D DATA FOR SUB-CRITICAL FLOW INTERACTING WITH VERTICAL JET	D-1

APPENDIX E. A POSSIBLE APPLICATION OF
SUB-CRITICAL FLOW JET INTERACTION

E-1.

LIST OF FIGURES

Figure Number		Page
2.1	Lay-out of Experimental Set-up	11
2.2	Jet Assembly	12
3.1	Rise at D/S for Small Q_j	24
3.2	Unsteady Rise for $Q_r = Q_{rc}$	24
3.3	Unsteady Hump	24
3.4	Unsteady Collapsed Hump	24
3.5a	Washed Collapsed Hump	24
3.5b	Flow Profiles for Super Critical Flow Interacting with a Vertical Jet	25
3.6	Steady Collapsed Hump for $Q_r \geq Q_{rc}$	24
3.7	Rise (in Stage II) for Small Q_j	26
3.8a	Separated Flow	26
3.8b	Flow Profiles for	27
3.9	Increased Air Bubble	26
3.10	Filled-up Bubble	26
3.11	Collapsed Filled Bubble	26
3.12	Reappearance of Air Bubble	26
3.13	Steady Collapsed Bubble	28
3.14	A-Jump Controlled Tail Water	28
3.15	B-Jump	28
3.16	C-Jump	28

Figure Number		Page
3.17	Plot of Discharge Ratio vs F_1 When Tail . Water not Controlled and D/S Flow is Super Critical	29
3.18	Plot of Sequent Depths vs Froude Number for A-Jump	30
3.19	Plot of F_1 vs Ratio of Bubble Length to y_1 (A-Jump)	31
3.20	Plot of y_{2B}/y_1 vs F_1 for B-Jump	32
3.21	Variation of Energy Loss with Froude Number in B-Jump	33
3.22	Variation of Length of Eddying Zone V/S F_1 in B-Jump	34
3.23	Variation of Hump Height with F_1 in B-Jump	35
4.1	Definition Sketch	43
4.2	Typical Water Surface Profiles for Different Discharge Ratios	44
4.3	Plot of Initial Froude Number vs Maximum Discharge Ratio	45
4.4	Variation of Q_r with F_j	46
E.1	Schematic Diagram of a Possible Application	E-3

NOTATIONS

The general suffix 1 and 2 indicates the upstream and down stream of the impingement zone.

B	width of the flume
b	jet thickness
E ₁	upstream specific energy
E ₂	downstream specific energy
E _j	energy of the jet = $\frac{V_j^2}{2g} = \frac{Q_j^2}{B^2 \cdot b^2 \cdot 2g}$
F ₁	upstream Froude Number
F ₂	down stream Froude Number
g	acceleration due to gravity
L _b	length of the air bubble
L _e	length of eddying zone
Q ₁	upstream horizontal discharge
Q _j	jet discharge
Q ₂	down stream horizontal discharge
Q _r	discharge ratio = $\frac{Q_j}{Q_1}$
Q _{ra}	discharge ratio corresponding to separation
Q _{rc}	discharge ratio for unsteady hump formation
Q _{rd}	discharge ratio for steady collapsed hump
V ₁	upstream mean velocity
V ₂	down stream mean velocity
V _j	velocity of the jet

y_1	upstream depth
y_{1A}	upstream depth in A-jump
y_2	down stream depth in A-jump
y_{2B}	down stream depth in B-jump
y_{hB}	hump height
ν	kinematic viscosity

ABSTRACT

The experimental investigation was aimed at *studying* the effect of a vertically upward issuing two dimensional jet interacting with a free surface flow in a channel. Both super-critical and sub- critical flows have been studied.

The critical discharge ratios for the transition of the flow situation and the flow profiles , for the super critical flow interacting with vertical jet have been studied. Also the energy loss and the sequent depth ratio have been compared with the classical jump and are satisfactory.

Flow profiles resulting from the interaction of a sub-critical flow with vertical jet are analysed. With some constraints, there is a drop formation and that can be utilised as a flow measuring device.

CHAPTER I

INTRODUCTION

Energy dissipating device is a main part of a hydraulic structure. The basic purpose of an energy dissipating device is to provide suitable transition from the higher velocities to normal low velocities of the natural stream.

The most widely used single means of energy dissipation is the hydraulic jump. The hydraulic jump can take place in an energy dissipating device in different forms (1) viz:

- (a) A hydraulic jump in a horizontal channel known as a classical jump.
- (b) Hydraulic jump at an obstruction as an abrupt rise, which is considered to be the best at present, as it reduces the stilling basin length.
- (c) Jump below a vertical drop of the floor:
in this case energy is dissipated by transfer of energy from the falling nappe to the circulating flow in the pool.

- (d) Jump at submerged outlet: the hydrostatic pressure of the down stream side acts against the flow, thus reducing the velocities at the outlet.
- (e) Jump on sloping beds: the energy dissipation here is more than in the horizontal channels for same basin length.
- (f) Forced hydraulic jump: this can be produced by employing certain types of obstructions like friction blocks, etc. The hydraulic jump formed and thereby dissipation of energy by friction blocks have been studied in detail by Rajaratnam (2).

In all the above cases the flow has been forced to produce a hydraulic jump in a controlled region. This control of hydraulic jump is achieved by means of solid baffles, blocks, and stilling basins.

It appears to be advantageous at least theoretically to achieve the same purpose by a fluid jet from the bottom of the channel spanning the width of the channel and issuing upwards in place of solid obstruction.

Only available relevant literature regarding using a fluid jet as an obstruction is of Faktorovitch (3). Faktorovitch has studied the interaction of super-critical flow in an open channel with a vertically upward issuing jet at bottom of the channel. He has classified the flow phenomenon according to the kineticity (square of Froude Number) of the flow before and after the interaction.

The classifications proposed by Faktorovitch, are:

- (a) Rapid-Rapid
- (b) Critical-Rapid
- (c) Submerged-Rapid
- (d) Rapid-Critical
- (e) Critical-Critical
- (f) Submerged-Critical
- (g) Rapid-Submerged
- (h) Critical-Submerged
- (i) Submerged-Submerged

where the first word defines the kineticity of the free-surface impinging flow, the second word the kineticity of the joint flow. The term critical determines the regime of the flow passing from a rapid into a tranquil state in the form of a hydraulic jump in a critical form.

The basic equation for conjugate depths in the region of flows impingement was derived by use of momentum equation as

$$\frac{1}{n_1} + \frac{n_1^2}{2} = \frac{(1+n_1)^2}{n_2} + \frac{n_2^2}{2} = \Theta(n) \quad (1)$$

where

$$n = h/h_{crh}$$

$$n_q = \frac{q_f}{q_h}$$

here h = the depth of flow

h_{crh} = critical depth of horizontal flow

q_f = specific discharge issuing outward from the slot

q_h = specific discharge of the horizontal impinging flow.

Suffix 1, 2 indicates upstream and downstream of impingement zone.

The theoretical plot of Equation 1 has been given by Faktorovitch, along with other experimental

results like variation of coefficient of energy dissipation with Froude Number.

While classifying the flow phenomenon in super-critical case according to the kineticity, the critical conditions have not been clarified by Faktorovitch. There is a range of kineticities in which the flow is not stationary and the hump formation takes place before the transition, which collapses and is washed down, and repeats periodically. This aspect would be very important in the use of such a device for energy dissipation as such critical range should be avoided in the use of interaction of the jets as energy dissipators. Since there is no clarification about the separation of the flow in his work, there is a need to verify and simplify, if possible, the various classifications of the flow.

The interaction of sub-critical flow with a vertical jet does not appear to have been studied by any investigator. At least ^{the} author is not aware of any work done in this field. In this aspect even though the energy dissipation is not a main consideration it would be interesting to study this phenomenon from an academic point of view.

An experimental investigation of the interaction of an open channel flow and a vertically upward issuing two dimensional jet at the bottom of the channel was conducted with the following aims:

- (a) To study the classification of flow suggested by Faktorovitch (3) and to simplify it if possible.
- (b) To study the effect of a vertically upward issuing jet at the bottom of an open channel with a sub-critical flow.
- (c) To analyse the critical discharges when there is transition of the flow regimes.

This experimental investigation was conducted in the Hydraulics Laboratory of ^{the} Civil Engineering Department at ^{the} Indian Institute of Technology Kanpur.

The details of the experimental set-up for this investigation are given in Chapter II. Chapter III gives the study of super-critical open channel flow interacting with a vertically upward issuing jet. In Chapter IV is presented the study of sub-critical open channel flow interacting with a vertically upward issuing jet at the bottom of the channel. The study is summed up and recommendations for further study are given in Chapter V.

CHAPTER II

EXPERIMENTAL SET-UP

The experimental set-up, as shown in Figures 2.1 and 2.2 was essentially a rectangular glass-walled flume 500 cm. long, 45 cm. wide and 100 cm. deep. The bottom of the flume was of smooth sheet of aluminium. There were two control gates, one at the upstream end, and one at the down stream end of the flume.

A jet of rectangular cross-section spanning the full width of the flume was installed at ^{the} bottom of the flume. The nozzle was streamlined.

The flume was supplied with water from a constant head overhead tank, through a 20 cm. pipe-line to the head-tank of the flume. The flow was controlled by a gate valve. Fine adjustment of the discharge could be made by means of two bypasses provided across the main line. The two bypasses were of diameter 8 cm. and 5 cm.

The discharge to the nozzle was through a pipe-line also from the overhead tank. The flow, before entering the nozzle passed through a rectangular tank at the bottom of the flume which acted as a plenum

chamber. The jet discharge was controlled by a gate valve.

The disturbances caused in the flow at the entrance to the head tank of the flume were stilled by wooden and steel grids. The transition from the head tank to the flume was streamlined.

Flow Measuring Devices

Water from the flume was conducted through an underground channel (53.5 x 53.5 cm.) to the sump. This underground channel was provided with a sharp crested weir at down stream end. The head over the weir was measured by means of a point gauge to an accuracy of 0.1 mm. The point gauge was fixed on an observation well. Weir was calibrated volumetrically with the help of an underground calibration tank. The weir equation obtained by calibration is

$$C_d = 0.63 + 0.08 H/P \quad (2)$$

where

C_d = Coefficient of discharge

H = Head over the weir

P = Height of the weir

and was used in all the discharge calculations.

The discharge to the nozzle was measured by the pressure difference created across an orifice plate installed in the supply pipe to the jet. The differential head could be read to an accuracy of 1 mm. on a mercury manometer.

Water profiles and depths were determined with the help of a point gauge with a least count of 0.1 mm., mounted upon a carriage.

Two sets of experiments were conducted

- (1) The super-critical flow, interacting with the two dimensional vertical jet (explained in Chapter III). The super-critical flow was created by means of a sluice gate upstream of the flume. Different gate openings were used to obtain a wide range of Froude Numbers. Gate openings were from 2.00 cm. to 8.00 cm. Also two jet thicknesses (1.40 cm. and 0.725 cm.) were used in the study.
- (2) The sub-critical flow interacting with a two-dimensional vertical jet (analysed in Chapter IV). Two jet thicknesses were used to see the effect of the thickness as a parameter.

All the experiments were carried out for a zero slope of the flume.

A typical experiment consisted of measurement of water surface profile, the discharges Q_j through the jet, and $(Q_1 + Q_j)$ at the down stream end of the channel. A total of 120 experiments were conducted.

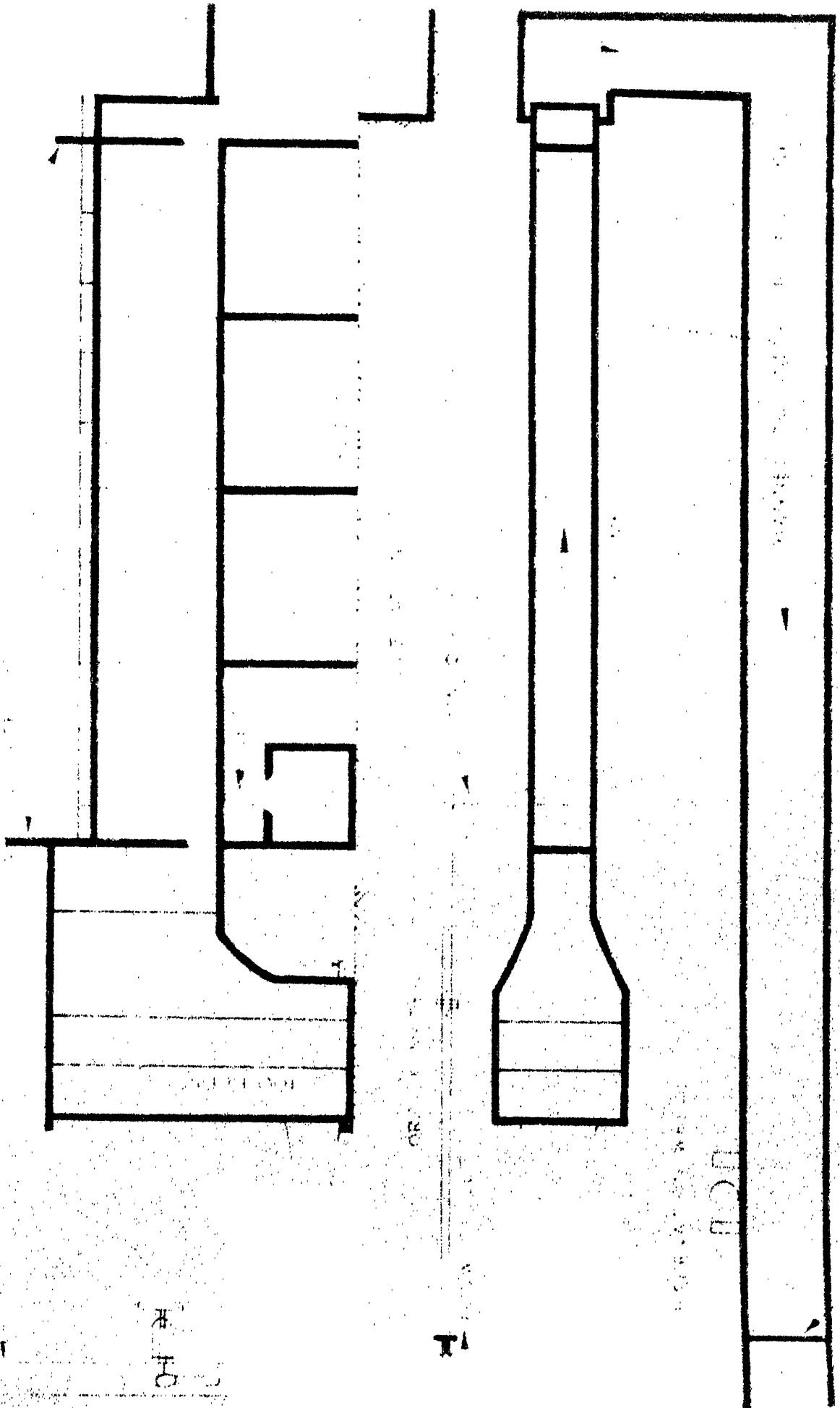
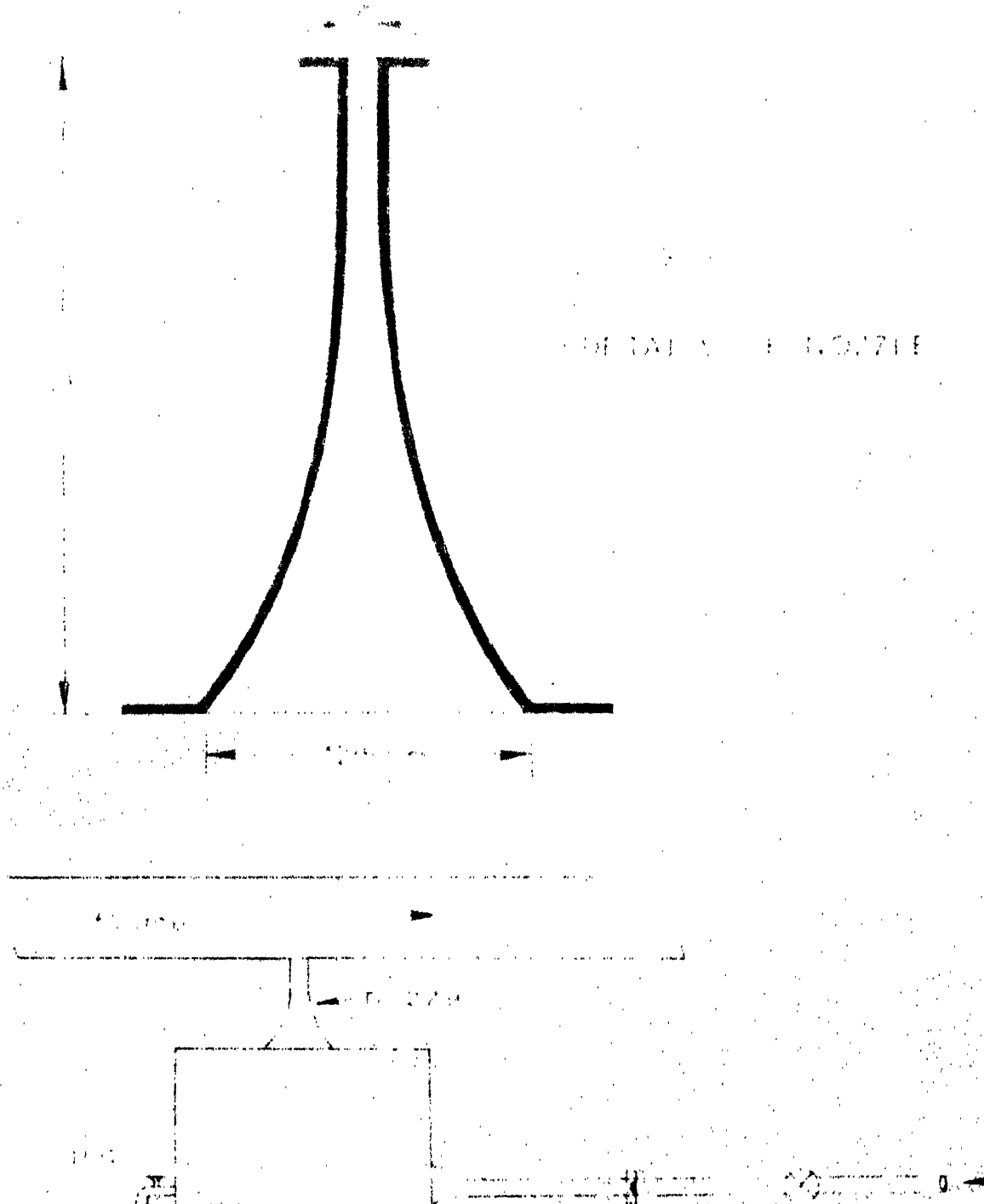


FIG. 2-1 LAY-OUT OF EXPERIMENTAL SET-UP



SCHEMATIC SKETCH OF LIFT ASSEMBLY

FIG 2.2 HT ASSEMBLY

CHAPTER III

INTERACTION OF SUPER-CRITICAL FLOW WITH A VERTICAL JET

3.1 Introduction

The experiments conducted on the super-critical flow interacting with the vertically upward issuing jet at the bottom of the flume, were of interest in finding out the energy dissipation and the flow profile characteristics. The tests were run in the glass walled flume explained in Chapter II. Experiments were performed for various discharge ratios $Q_r (= Q_j/Q_1)$, different gate openings thus varying the Froude Number, and different jet widths. Range of the parameters investigated is given in Table I. Detailed data are given in Appendix-A.

Table I - Range of the Parameters investigated for super-critical flow interacting with a vertical jet

Parameters	Range
Froude Number $F_1 = V_1 / \sqrt{g y_1}$	1.80 to 10.00
Discharge Ratio $Q_r = Q_j / Q_1$	0.10 to 0.70
B/b = Width of the flume/Jet thickness	32 and 63

3.2 Observations

Careful observations of the flow profiles for different discharge ratios revealed the following basic type of flow situations:

3.2.1 Stage I:

By allowing a discharge Q_1 to flow in the flume below a sluice gate with depth y_1 ($F_1 > 1$, super-critical flow), and if

- (a) small jet discharge Q_j is injected, the depth down stream of the jet is increased as shown in Fig. 3.1.
- (b) by further increasing the jet discharge Q_j for same Froude Number F_1 the down stream depth goes on increasing and at a particular value of the the jet discharge, there is a hump formation at the jet Fig. 3.3. This hump formed collapses Fig. 3.4, and a hydraulic jump is formed at up-stream of the jet. The collapsed hump was washed down by the super-critical flow and the profile resumes the original shape Fig. 3.5. Again the hump formation will reappear and again it will collapse and ^{get}washed down. This cycle of hump formation and collapsing continued for this

particular jet discharge ratio. The cycle is shown in Fig. 3.2 to 3.5. A typical plot of the profile is shown in Fig. 3.5b.

- (c) with further increase in jet discharge, it was observed that at a second particular value of jet discharge Q_{rd} the collapsed hump could not be washed down and the profile remains as in Fig. 3.6.

The above phenomenon was observed until the discharge Q_1 has reached (hence Froude Number F_1) a critical value. Beyond this value a new class of the formation of flow profiles was observed. The Froude Number corresponding to this first stage was approximately 4.0.

3.2.2 Stage II - Separation of the flow:

With F_1 greater than 4.0 if a

- (a) small jet discharge was injected, the downstream depth of the flow was increased Fig. 3.7.
- (b) with further increase in the jet discharge the flow separates (corresponding discharge ratio is Q_{ra}) at the downstream of the jet and an air bubble is formed Fig. 3.8a. A typical profile of the run is shown in Fig. 3.8b.
- (c) if the jet discharge is increased further and

further the air bubble formed increases in size and the profile is like a projectile of a thrown particle. The bubble formed will be filled up with water and then, there is formation of a hump and it collapses. At this discharge ratio Q_{rc} the collapsed hump is washed down and again the bubble is formed. This cycle continues. A cycle of formation of bubble, hump, collapsing hump and again bubble formation is shown in Figures 3.7 to 3.12.

- (d) with a further increase in the jet discharge, the air bubble formed is filled up with water, it collapses and remains collapsed and could not be washed down by the upstream super-critical flow Fig. 3.13 the corresponding discharge ratio for which the collapsed hump is steady is Q_{rd} .

In all the above cases except the one in which bubble formation takes place, the down stream flow was super-critical and no attempt was made to change the tail water depth.

3.3 Stage II - Varying depth of tail water:

In the case when aeration starts, the tail water depth was controlled by a sluice gate. The different profile

observed with increasing tail water depth has been classified as type A, type B and type C jump. The reason for studying only this case with controlled tail water depth is that, this is the region of practical interest as most of the hydraulic structures needing the energy dissipation works have higher Froude Number (>4.0). If interacting jets are to be employed for energy dissipation then the discharge injected should be the minimum possible to have desired effects. The observed profiles are given below:

3.3.1 Type A Jump:

After the formation of the bubble the tail water depth is increased such that a hydraulic jump is formed between the tail gate and the place where the combined jet hits the floor as shown in Fig. 3.14. The two depths y_{2A} and y_{1A} were measured to compare the sequent depth ratio with that of classical hydraulic jump. The length of the bubble was also measured.

3.3.2 Type B Jump:

With increased tail water depth the toe N of the hydraulic jump approaches M Fig. 3.14 and then the air bubble formed is filled up with water. At this critical depth of tail water the filled bubble, the eddying zone, starts collapsing and it is classed as type B, Fig. 3.15.

The tail water depth y_{2A} was measured for the known discharge ratios.

3.3.3 Type C Jump:

If the tail water depth is increased beyond that of type B formation as above, then the hump (i.e. filled up bubble or eddying zone) collapses and a submerged hydraulic jump is formed upstream of the jet and downstream of the sluice gate Fig. 3.16. The tail water depth was further increased to get the different submergences.

3.4 Analysis

The variation of the discharge ratios required to cause a transition from one flow situation to another was studied. These critical values of Q_r were found to be the functions of Froude Number F_1 only.

To study this Q_{ra} , Q_{rc} , and Q_{rd} (critical value of discharge ratio at which flow situation changes) is plotted against Froude Number F_1 in Fig. 3.17. From a study of this Figure the following interesting points are observed:

- (a) for Stage I the hump formed at the jet starts collapsing (unsteady) for a critical discharge Q_{rc} shown by curve B and is collapsed (steady)

when the discharge ratio Q_{rd} reaches another critical value given by curve C.

- (b) it is seen that separation of flow takes place when i.e., stage II starts, when $F_1 = 4.0$ and the discharge ratio is about 0.25. For higher Froude Number F_1 the discharge ratio Q_r is fairly constant for the starting of separation.

In general the critical discharge ratios Q_{ra} , Q_{rc} and Q_{rd} corresponding to (i) separated flows (curve A) (ii) hump collapsing (unsteady case Curve B) (iii) collapsed hump (steady case curve C) are dependent only on F_1 . The jet width i.e., $(b/y_1$ or $B/b)$ does not have any effect on the phenomenon.

The difficulty of observation of the critical stages exactly is believed to be responsible for the scatter of data in Fig. 3.17. However, the trend is easily discernable.

It is to be noted that the three types of jumps studied here viz. A, B and C correspond to the minimum discharge ratio, Q_{ra} which causes a separation of the super-critical flow. Hence there can be other jumps of these categories also, for discharges $Q_r > Q_{ra}$, where Q_{ra} is discharge ratio which causes separation of an on

coming flow as given in Fig. 3.17 (curve A). These jumps can be called as A^+ , B^+ and C^+ jumps. The jumps A, B and C were selected for study as these give the value of minimum jet discharge needed to achieve the desired energy dissipation.

3.4.1 Sequent depth ratio and Froude Number in A-Jump:

The analysis of the controlled tail water depth in the critical region when the separation starts, shows that the plot of sequent depth ratio vs. the Froude Number for type A-jump is same as that of a classical jump Fig. 3.18. Plot of ratio of the L_b/y_1 vs F_1 shows a unique relationship which is linear Fig. 3.19.

Sequent depth ratio and Froude Number for B-Jump:

y_2B/y_1 vs F_1 is plotted in Fig. 3.20. It is seen that sequent depth ratio varies linearly for, all practical purposes, with F_1 . As noted before since B-jump corresponds to Q_{ra} , which is a function of F_1 (Fig. 3.17), the discharge ratio Q_r does not enter as a third parameter. If however jumps of this category which $Q_r > Q_{ra}$ i.e., B^+ jumps are studied then the sequent depth ratio for them would be a function of F_1 and Q_r . Fig. 3.20 shows a line corresponding to the classical jump also. The reduction in the sequent depth ratio for B-jump is seen to be 10 to 20%.

Energy dissipation in B-Jump:

The energy dissipation in the jump ΔE

$$\Delta E = E_1 + E_j - E_2$$

where the suffix 1, 2 and j refer to the beginning of the jump, the end of the jump and the jet respectively. The non-dimensional energy ratio

$$E_{IR} = (E_1 + E_j - E_2) / (E_1 + E_j)$$

is plotted against F_1 in Fig. 3.21. It is interesting to note that the energy loss ratio E_{IR} is same as in the classical jump, given by a well-known expression (2)

$$(E_1 - E_2)/E_1 = (\eta - 1)^3 / 4\eta$$

$$\text{where } \eta = \frac{1}{2} (\sqrt{8 F_1^2 + 1} - 1) \quad (1)$$

Advantages of B-Jump:

The advantages of the B-jump as an energy-dissipating device is apparent from Fig. 3.20 and 3.21. For a given Froude Number F_1 the B-jump can give the same amount of energy dissipation as a classical jump but with a marked reduction in tail water depth. Also the position of the B-jump is controlled in the sense

that the location of the hump and the jump are fixed in position relative to the jet position.

The length of the eddy zone which is important for the design of stilling basin length is found to be a function of F_1 and y_1 and is shown plotted in Fig. 3.22.

The hump height y_{hB} is generally larger than y_{2B} and its variation is studied and has been given in Fig. 3.23.

3.5 Conclusion

Since the present study was of exploratory in nature, the other characteristics of the jump essential for the design, like the length of the jump the shear stresses on the bed and velocity distribution were not studied. However, it is apparent from the above study that the phenomenon of the action of vertical jet on supercritical flow is similar to that of a forced hydraulic jump (2). The vertical jet which acts like a flexible baffle could be called as "Water Baffle". However, water baffles have an advantage over the solid baffles that these could be controlled (by adjusting the jet discharge) to suit the upstream and tail water flow conditions.

Though the case studied was only of a minimum discharge which will just separate the flow, it is logical

to assume that higher discharge ratios i.e. B^+ jumps will give a better control of the tail water and at least the same amount of energy dissipation as that of the classical jump if not more.

Finally it can be concluded that the water baffle has high potentialities to be developed as an energy-dissipating device. Further detailed studies on various aspects of B-jump and B^+ jumps ~~are~~ needed.

The effect of inclined jet needs study, C-jump has not been studied and needs a careful and detailed study.

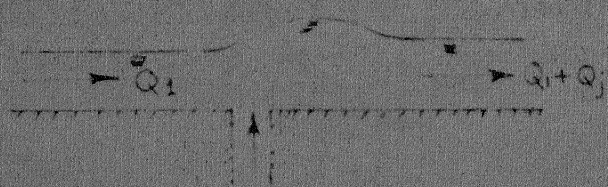


FIG. 3.1 RISE AT C/S FOR
SMALL Q_r

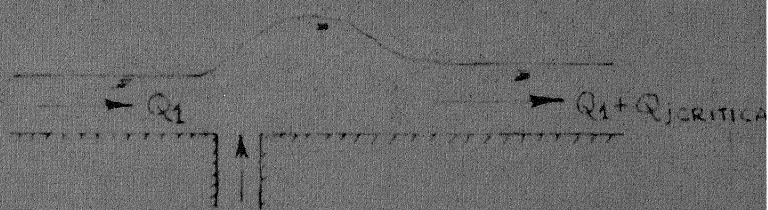


FIG. 3.2 UNSTEADY RISE
FOR $Q_r = Q_{rc}$

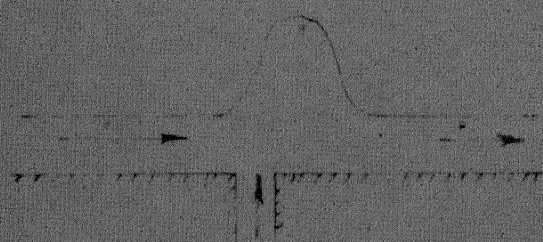


FIG. 3.3 UNSTEADY HUMP

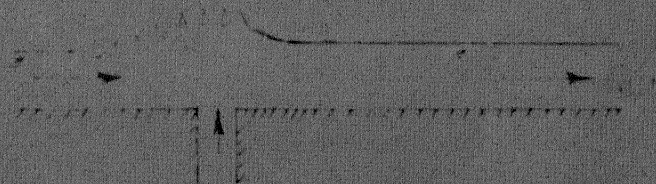


FIG. 3.4 UNSTEADY COLLAPSED
HUMP

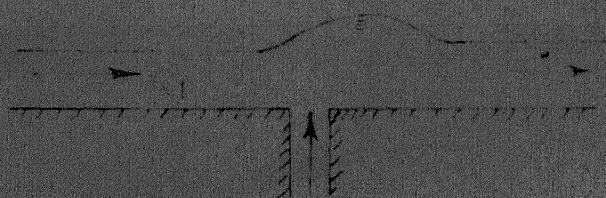


FIG. 3.5a WASHED COLLAPSED
HUMP

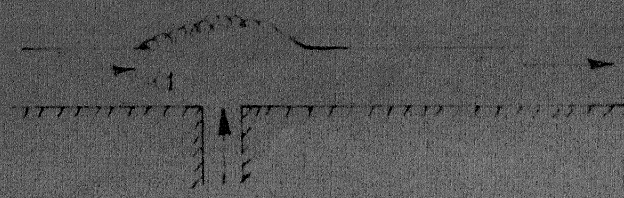


FIG. 3.6 STEADY COLLAPSED HUMP
FOR $Q_r > Q_{rc}$

70

30

30

0

0

PROFILE A WHEN HUMP FORMED IS COLLAPSED FOR

$F = 3.50$, $Gr = 0.22$

PROFILE B WHEN FLOW SEPARATES FOR

$F = 2.28$, $Gr = 0.32$

base Deflection
curves

collapsed

AIR

E

A

40

80

120

160

x in cm

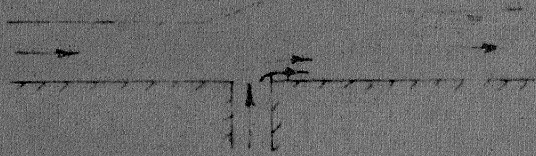


FIG. 3.7 RISE (IN STAGE II) FOR SMALL Q

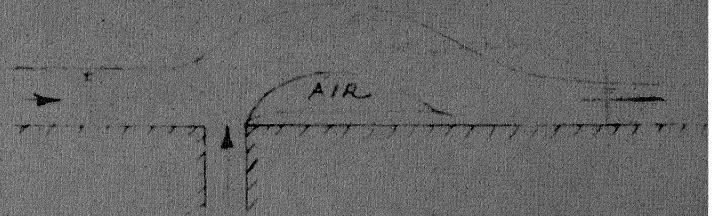


FIG. 3.8a SEPARATED FLOW

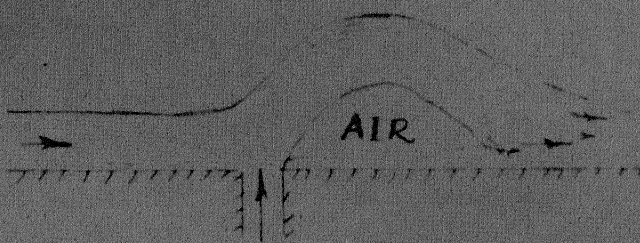


FIG. 3.9 INCREASING AIR BUBBLE

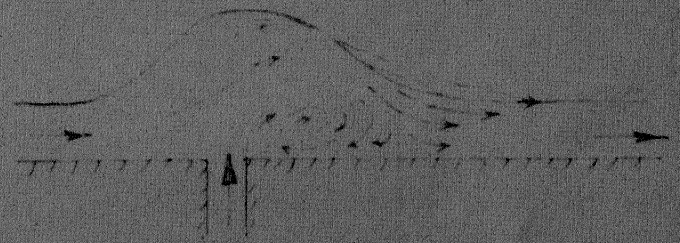


FIG. 3.10 FILLED-BUBBLE

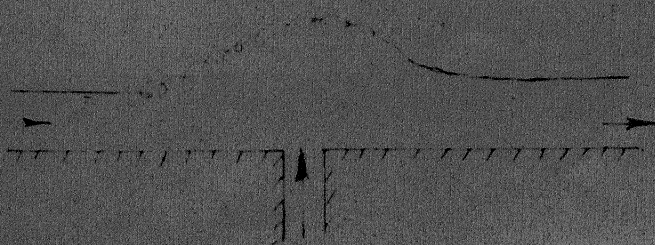


FIG. 3.11 COLLAPSED FILLED BUBBLE

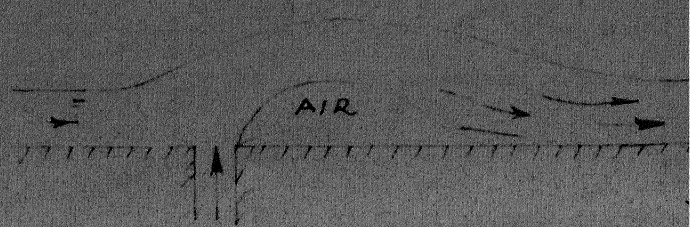
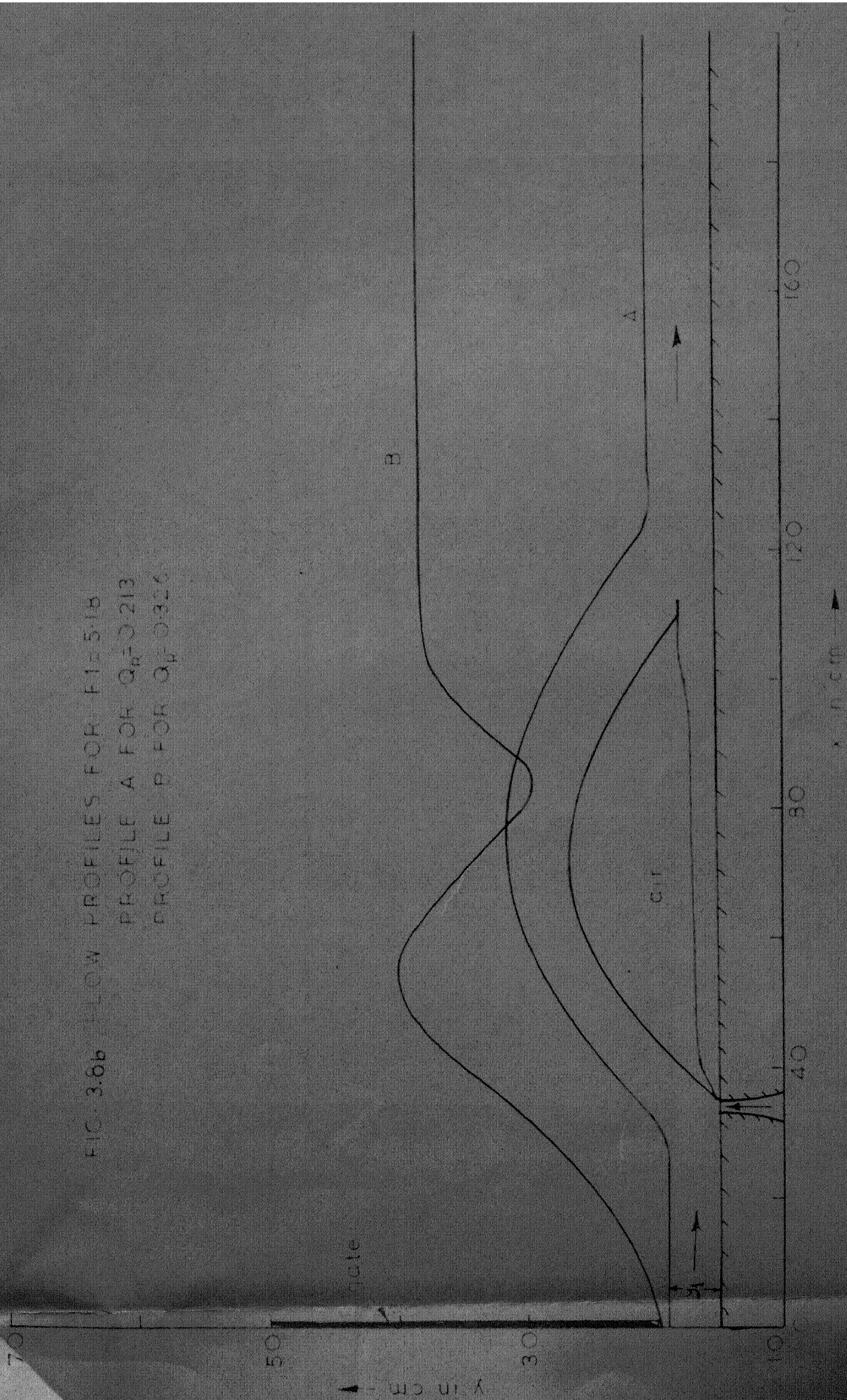


FIG. 3.12 REAPPEARANCE OF AIR-BUBBLE

FIG. 3.8b FLOW PROFILES FOR $F1=5.18$
 PROFILE A FOR $Q_0=0.213$
 PROFILE B FOR $Q_0=0.326$



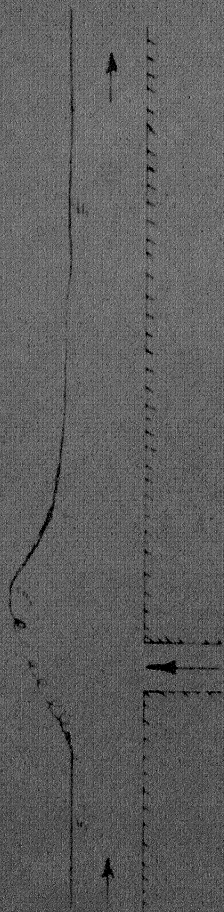


FIG. 3.13 STEADY COLLAPSED
BUBBLE



FIG. 3.14 A-JUMP (CONTROLLED
TAIL WATER)

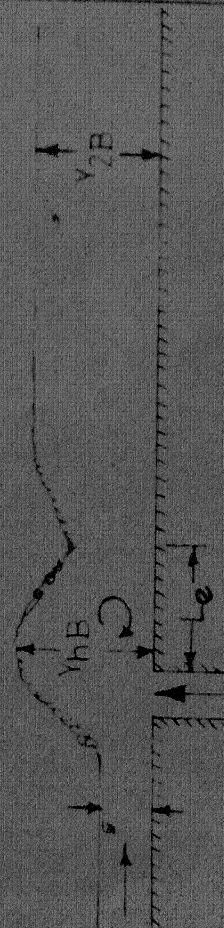


FIG. 3.15 B-JUMP

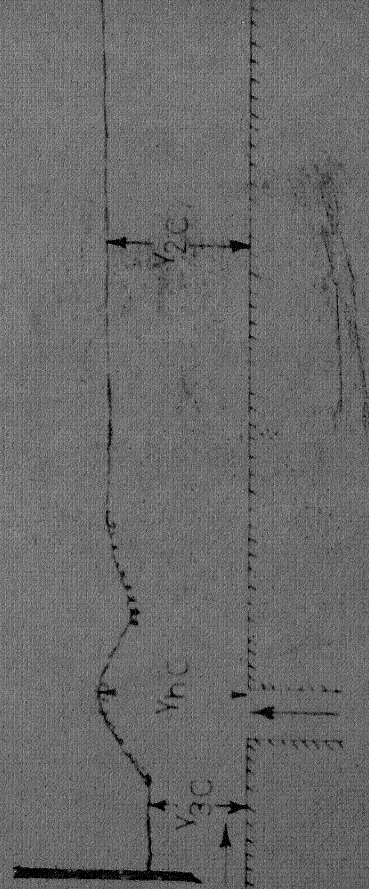


FIG. 3.16 C-JUMP

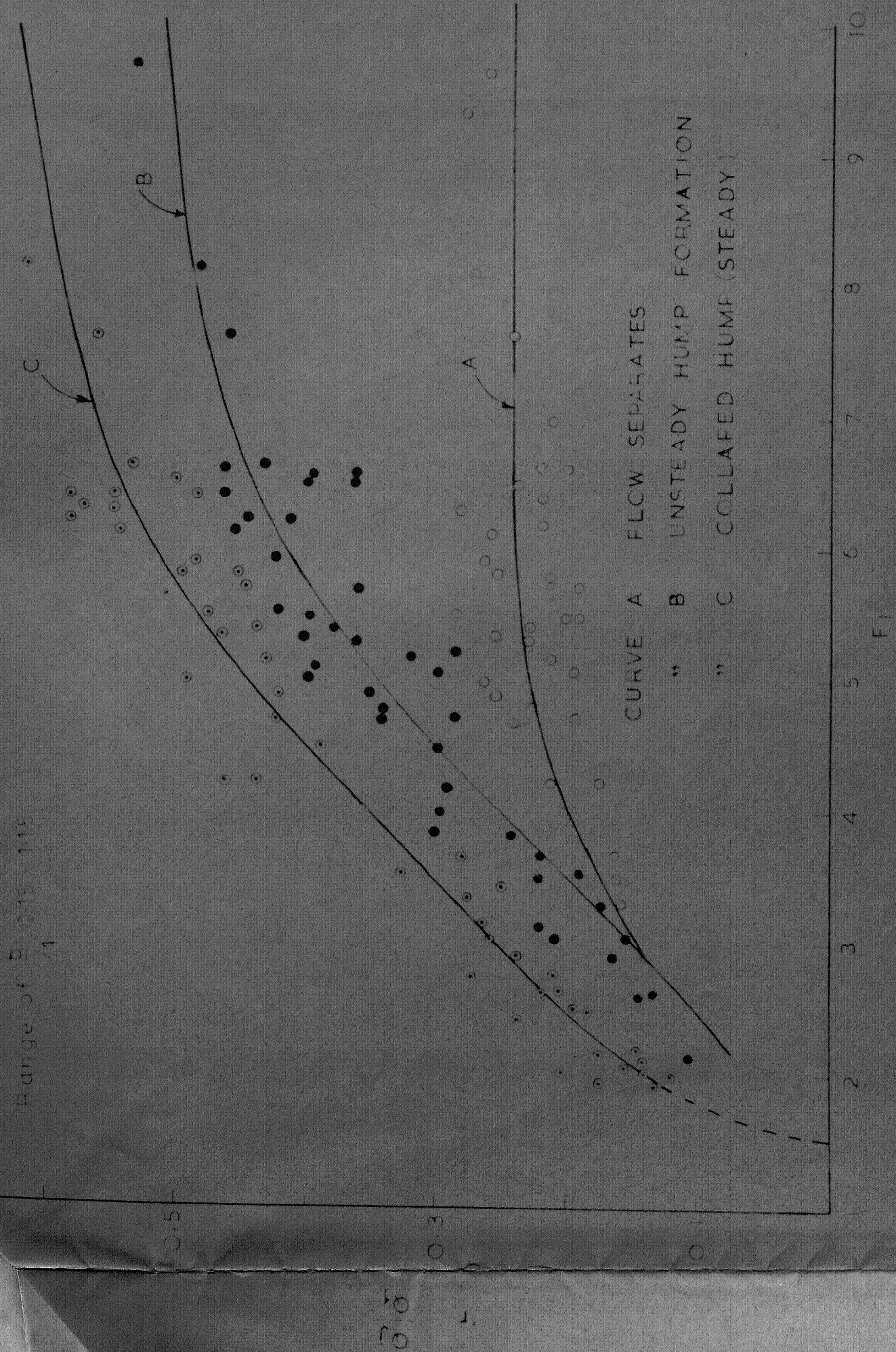


FIG. 317 PLOT OF DISCHARGE RATIO VS F_1 WHEN TAIL WATER NOT CONTROLLED AND $1/5$ FLOW IS SUPER CRITICAL

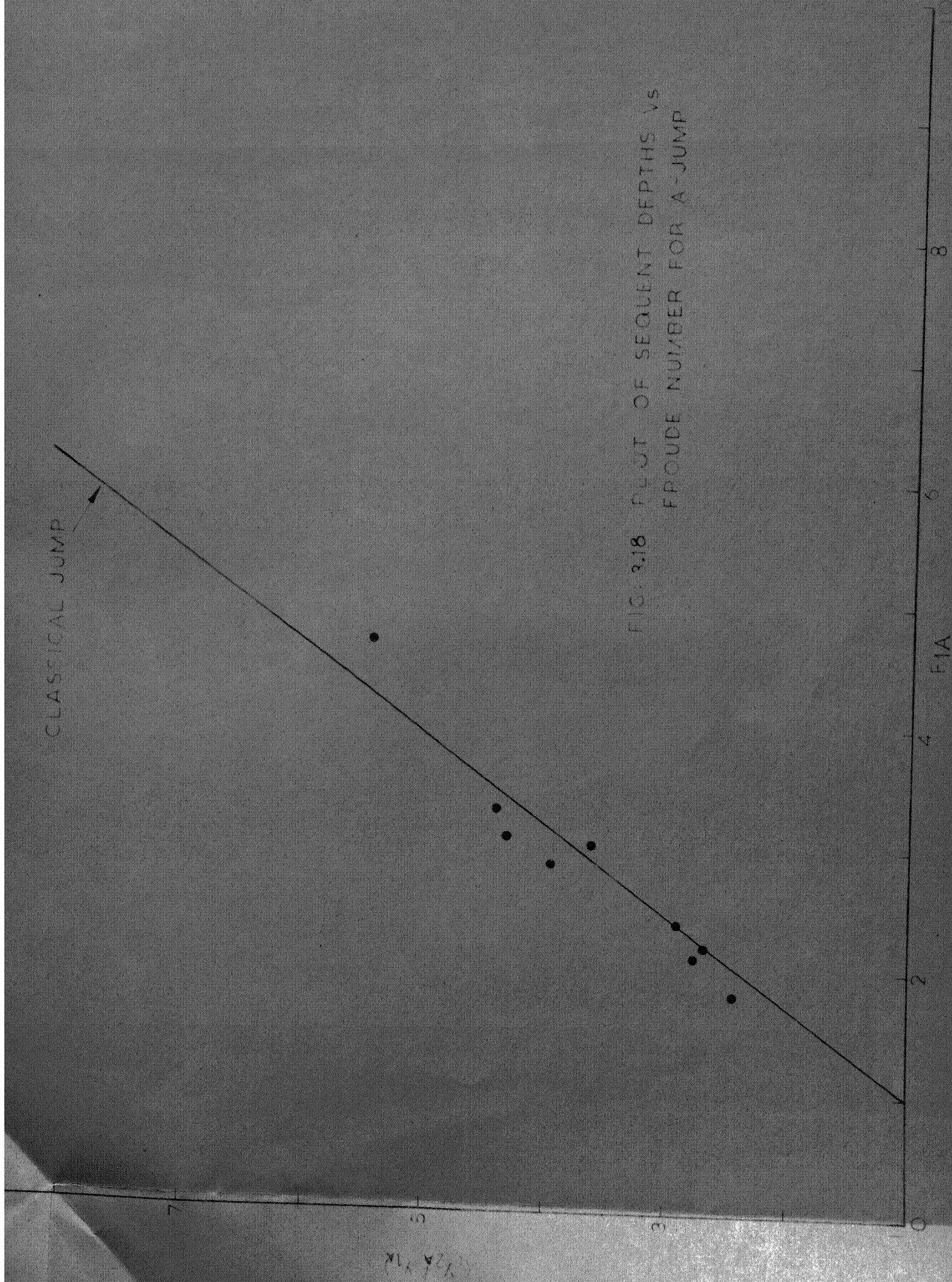
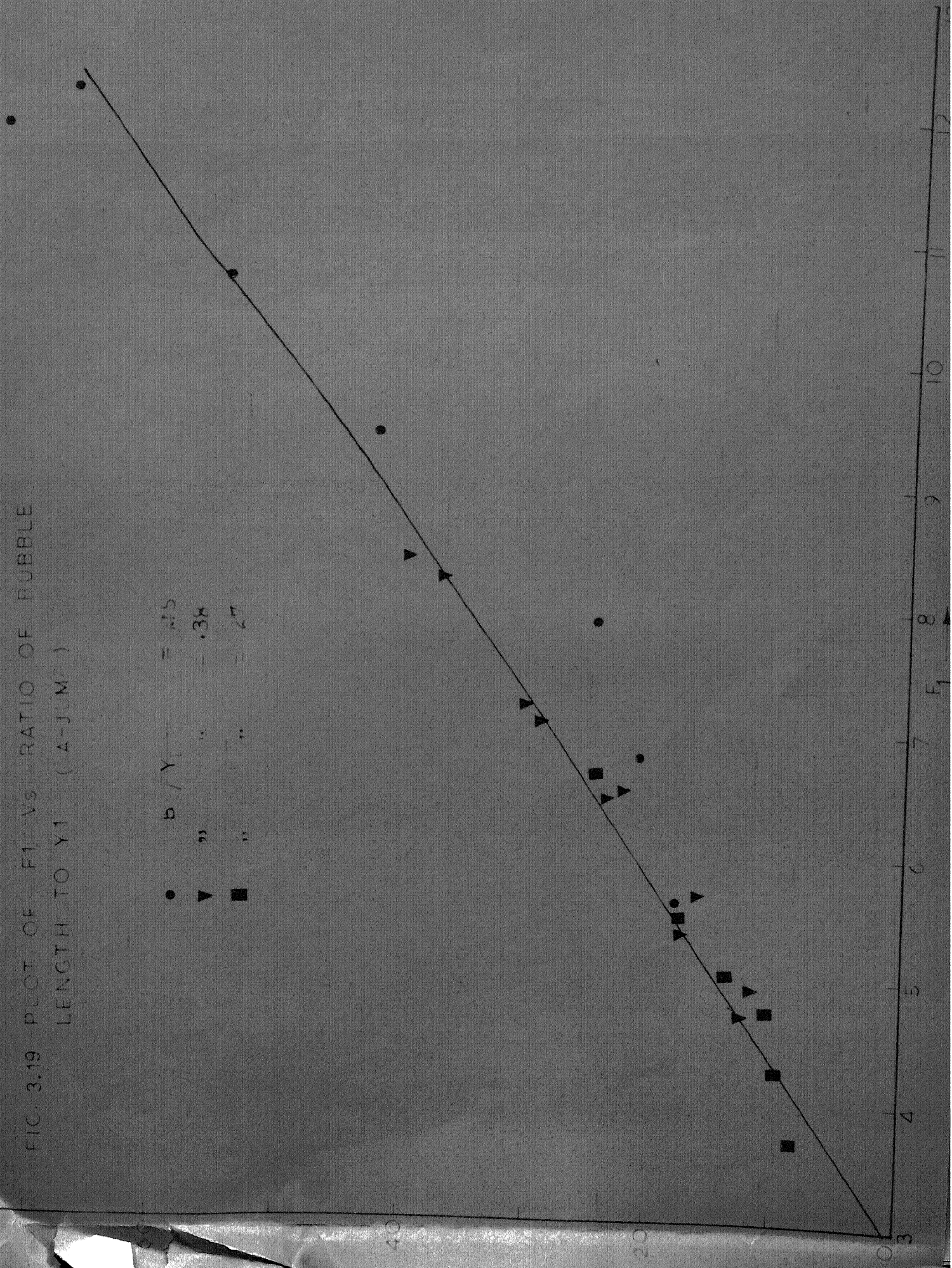
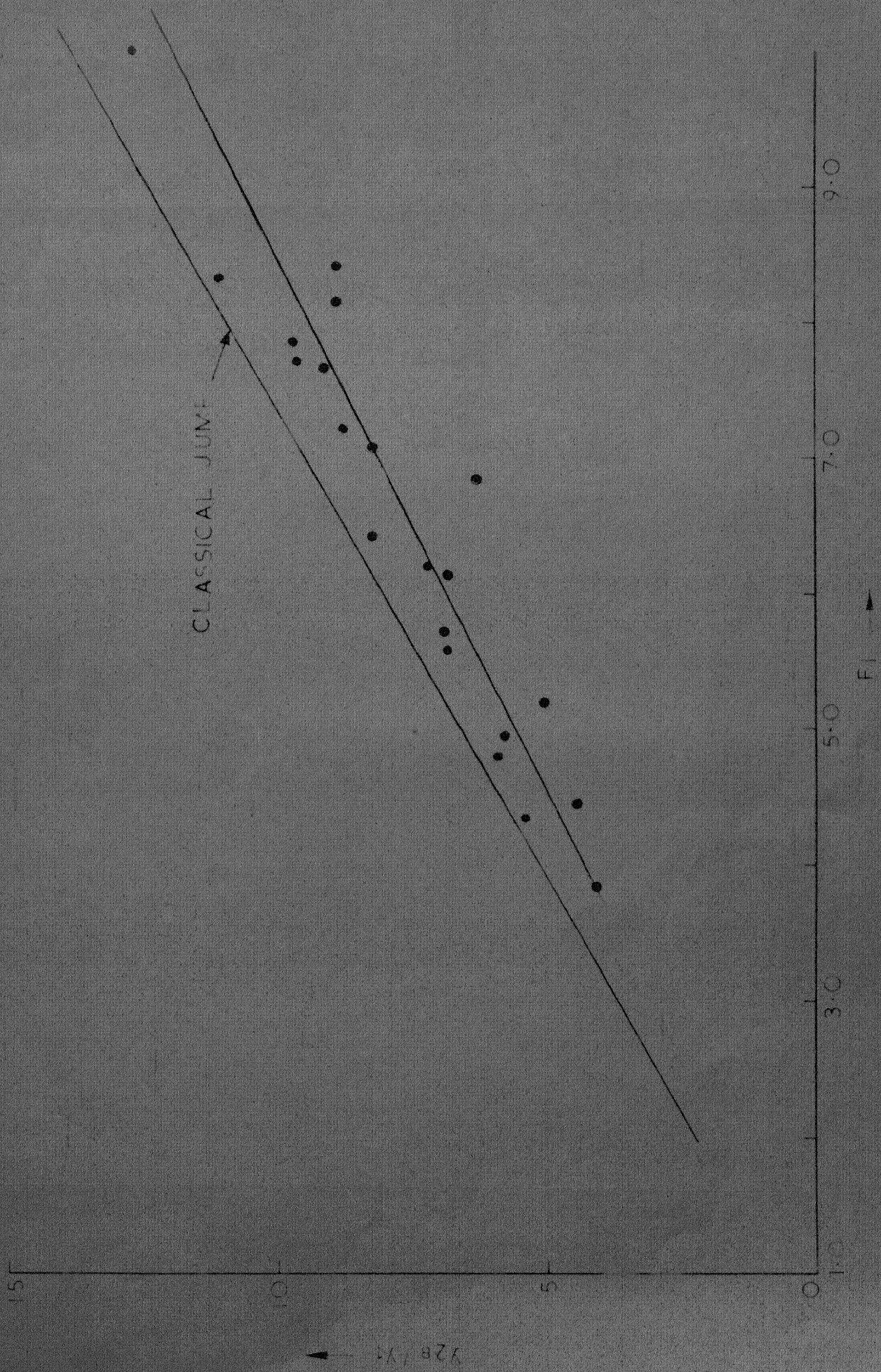


FIG. 3.19 PLOT OF F_1 VS. RATIO OF BUBBLE
LENGTH TO Y_1 (Δ -JUM)

\bullet $b/Y_1 = .15$
 \blacktriangledown " " $= .35$
 \blacksquare " " $= .5$



FIG. 3.20 PLOT OF Y_{2B}/Y_1 VS F_1

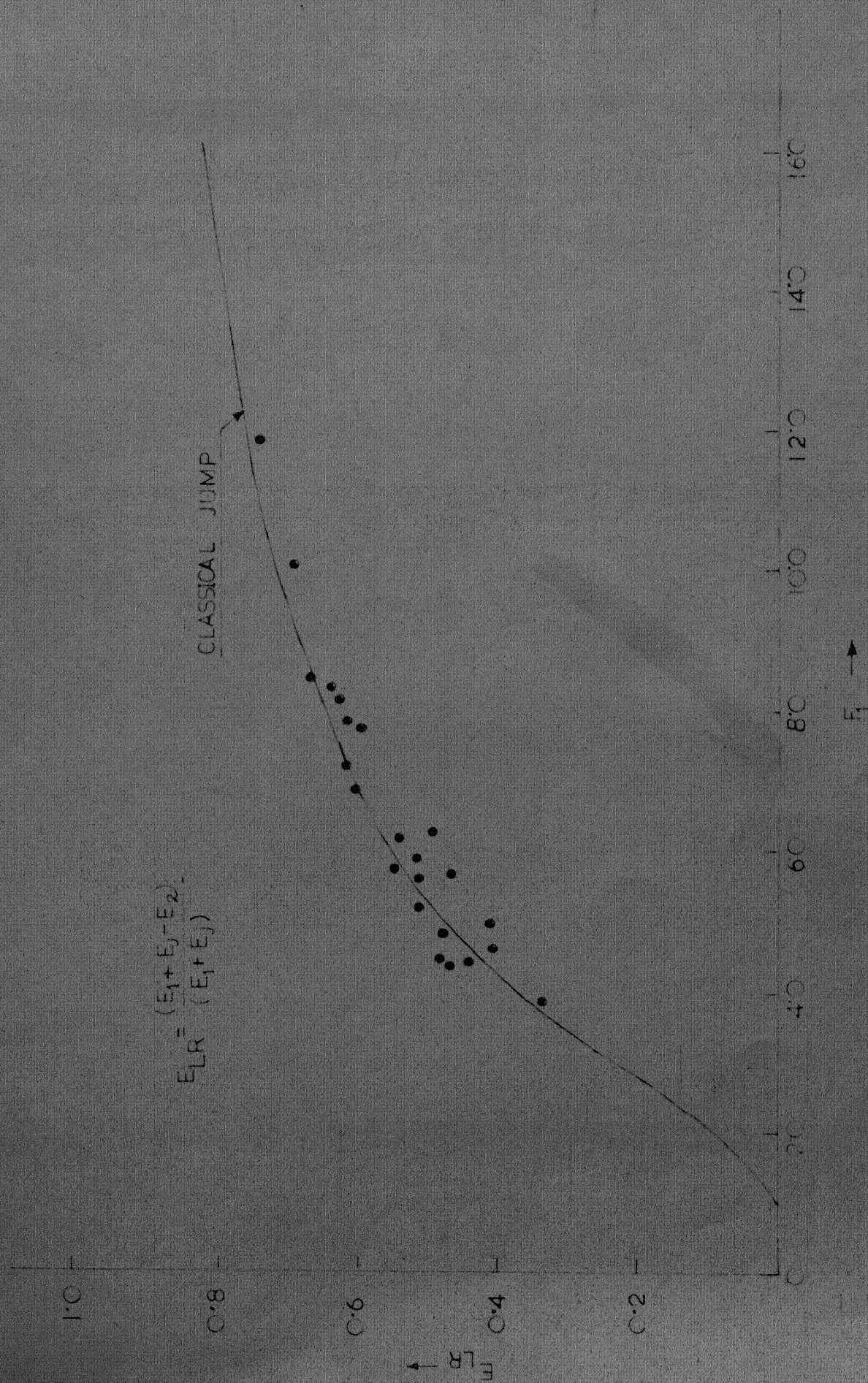


FIG. 3.21 VARIATION OF ENERGY LOSS WITH FROUDE NUMBER IN B-JUMP

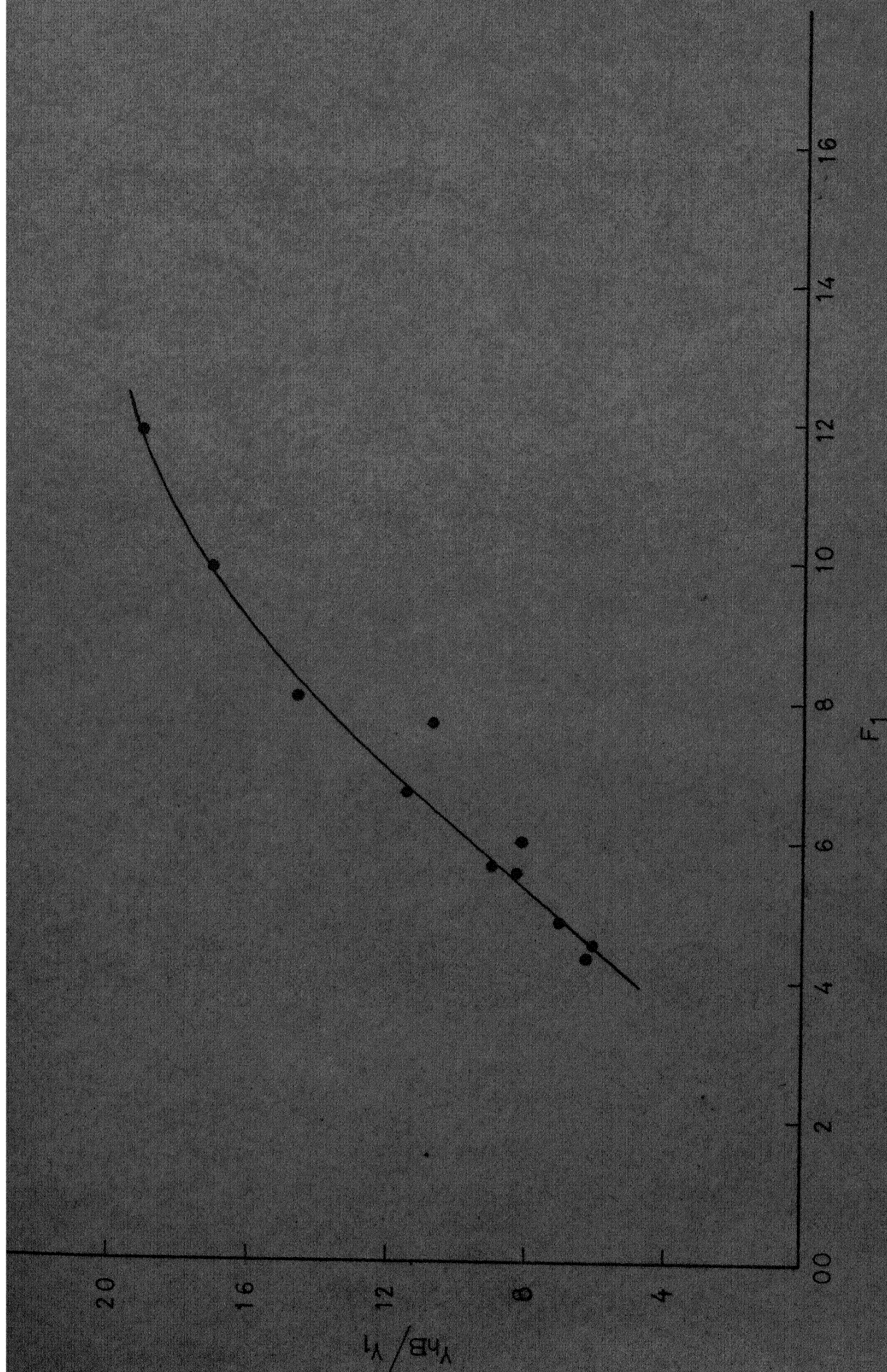


FIG. 3.23 VARIATION OF HUMP HEIGHT WITH F_1 IN B-JUMP

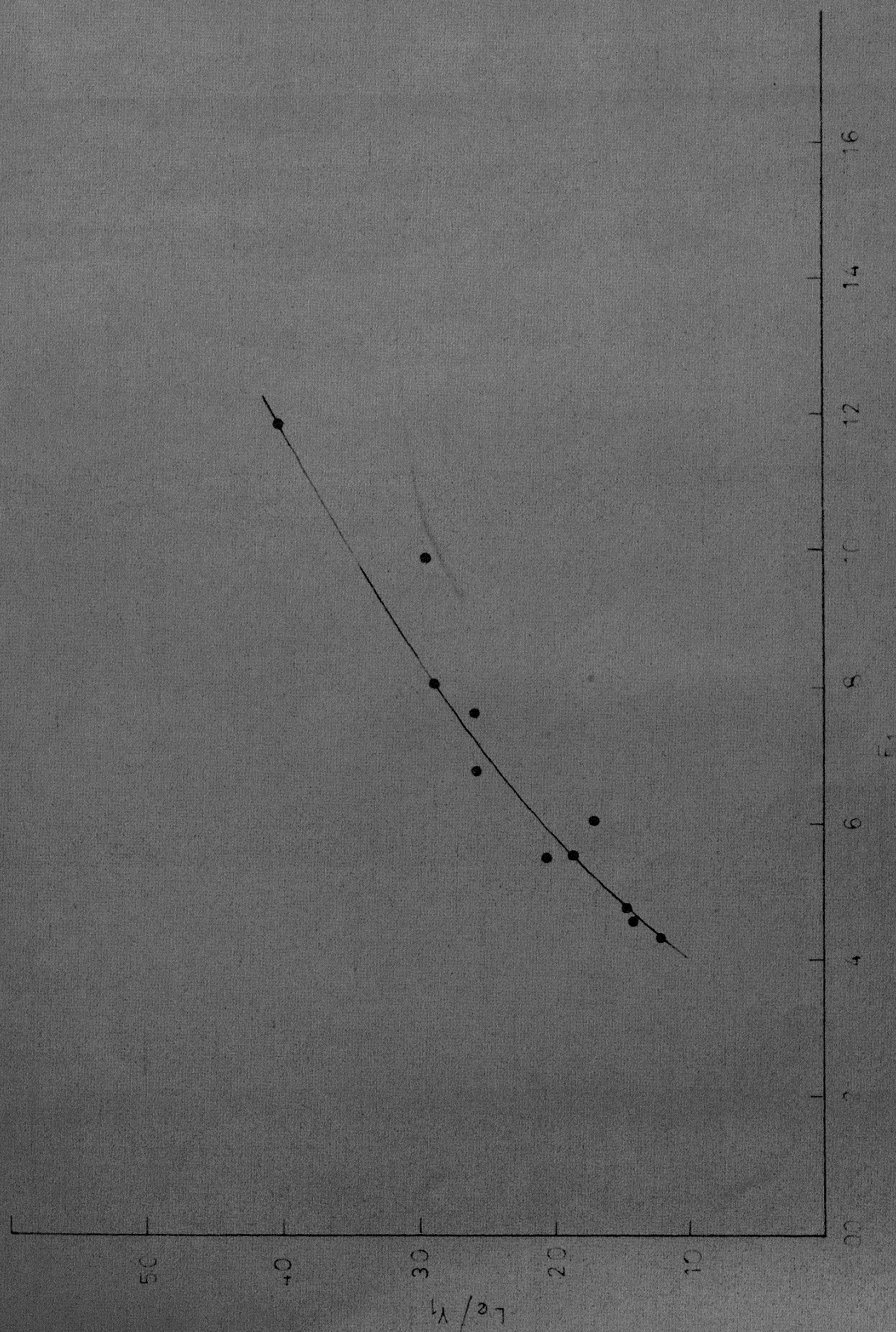


FIG. 3.72 VARIATION OF LENGTH OF EDDYING ZONE VS F_1
IN B-JUMP

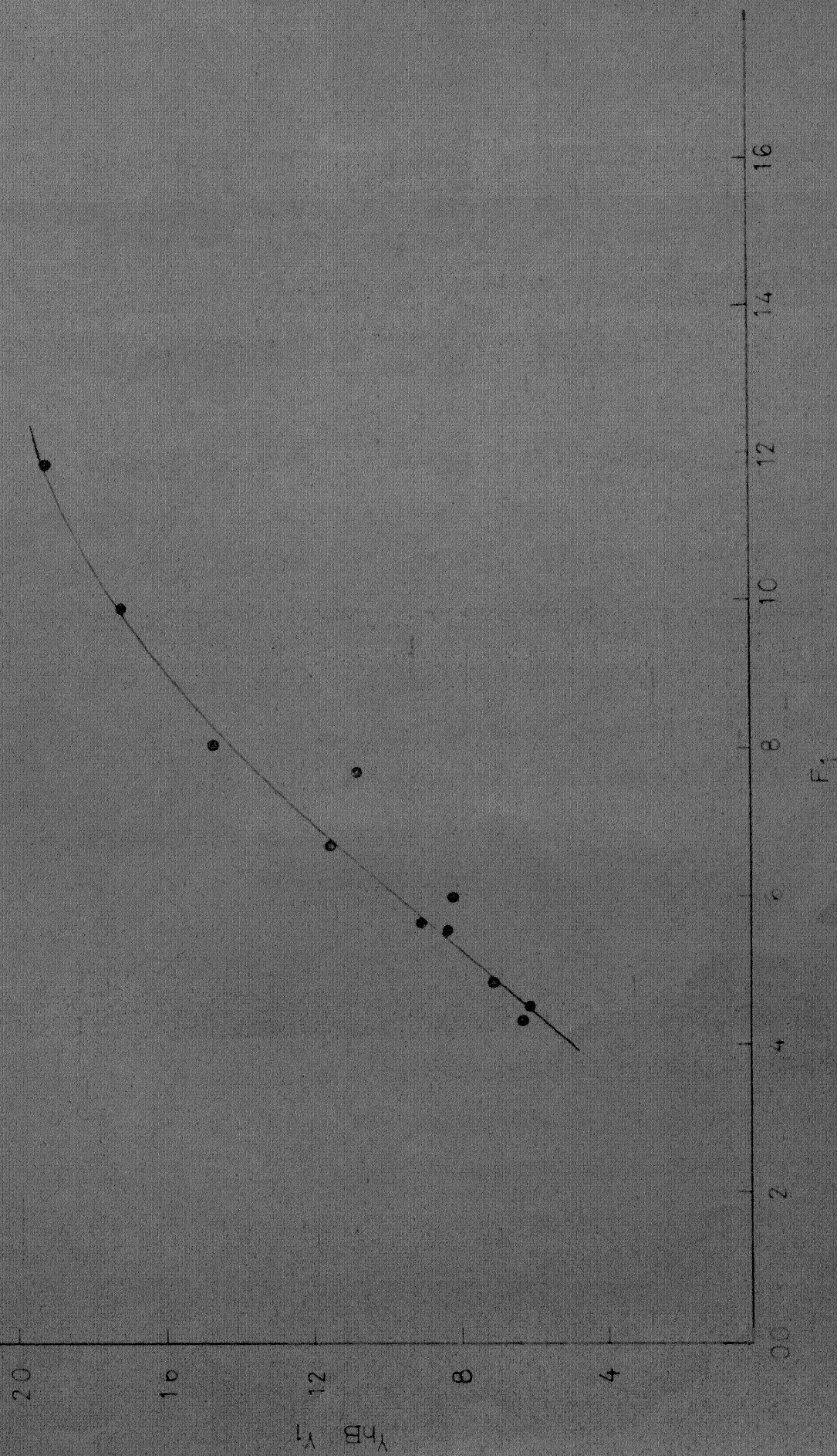


FIG. 3.23 VARIATION OF HUMP HEIGHT WITH F_1 IN B-JUMP

CHAPTER IV

SUB-CRITICAL FLOW INTERACTING WITH VERTICAL JET

4.1 Introduction

The interaction of a two dimensional jet, injected vertically up at the bottom of a free surface flow is of considerable importance in employing it as an energy-dissipating device. It has been reviewed in previous chapter, when the free surface flow is super-critical.

However no information is available on the action of a vertical jet on a sub-critical open channel flow. Here is presented a study of the interaction of the sub-critical flow with a vertical jet with a view to fill in this lack of information.

4.2 Experimental Observations

An experimental investigation was conducted to study the effect of a two dimensional vertical jet on a sub-critical flow. The experimental set-up explained in Chapter II was employed. Experimental data were collected for various discharge ratios Q_r and different slot widths. The range of the parameters studied is given in Table II.

Table II - Range of the parameters studied for sub-critical flow interacting with vertical jet.

Parameters	Range
Initial Froude Number	
$F_i = q_1 / \sqrt{g y_i^3}$	0.40 to 0.90
Discharge Ratio	
$q_r = q_j / q_1$	0.05 to 0.80
$B/b = \frac{\text{Bed width}}{\text{Jet thickness}}$	32 and 63

The first part of the investigation was concentrated on the description and ~~classification~~ of the interaction phenomenon. As a result of careful study of the experimental observations, the following changes of the water surface elevations were observed.

4.2.1 Change in Surface Elevation Observed:

When a small discharge Q_j is injected upward, from a nozzle spanning the full width at the bottom of the channel, on to a sub-critical flow with depth y_i and discharge Q_1 , the jet gets deflected by the cross flow

and the additional momentum input into the system causes a differential level to develop. The action of a jet on the water surface is similar to that of a hump on the bed of a channel. As well the increase in the unit discharge in the channel has an effect on the water surface similar to that of reducing the channel width.

4.2.2 Formation of the Drop:

As the jet discharge Q_j is increased, after a critical value $Q_{r \min} = Q_j/Q_1 = 0.05$ to 0.2 , the water surface undergoes a change and resembles that of a hydraulic drop Fig. 4.1. The flow can be divided into two distinct regions;

- (a) Upstream sub-critical flow and a down stream super-critical flow: the critical depth will occur in the curved portion of the drop, probably at the point of inflexion of the water surface profile.
- (b) Depending on the down stream control, the down stream flow will consist of (a) completely super-critical flow as explained in (a), (2) a free hydraulic jump or (3) submerged jump. Fig. 4.2 shows the typical water surface profiles obtained in a typical run, for various $Q_r (= Q_j/Q_1)$ values.

4.2.3 Surface Penetration by Jet:

If the jet discharge is further increased, the hydraulic drop type of water surface profile will continue till an upper critical value of Q_r is reached. For all these discharge ratios the flow upstream of jet will be sub-critical and ^{on}down stream super-critical. At this upper value, the jet will have relatively higher momentum and will penetrate the sub-critical flow. The water surface will become very rough in the curved portion because of splitting of the jet. The value of discharge ratio ($Q_{r \text{ max}}$) corresponding to this phenomenon to occur was in the range 0.5 to 0.9, and depends upon the initial Froude Number of the flow. Fig. 4.3 gives a plot of $Q_{r \text{ max}}$ vs F_i . All the experimental data have been plotted. A general trend in the decrease of $Q_{r \text{ max}}$ with F_i can be easily seen. The scatter of data is due to experimental difficulty of finding $Q_{r \text{ max}}$ precisely.

4.3 Analysis

Considering the situation where Q_r is such that a hydraulic drop is formed with a super-critical down stream flow; the depth of flow upstream of the jet, y_1 , will be independent of y_2 and will be given by

$$y_1 = \text{fn} (Q_1, Q_j, B, b, g, \gamma) \quad (4.1)$$

control were such, as to produce a hydraulic drop.

Fig. 4.4 shows a plot of Q_r vs. F_j for all the experimental data. It is clearly seen that all the data lie on a single curve. There is no effect of either the initial Froude Number F_i or the thickness of the jet. The small scatter of the data is due to observational errors. Thus for a hydraulic drop case, Equation 4.3 can be written as

$$F_1 = \text{fn} (F_j) \quad (4.5)$$

4.4 Applications

The formation of a hydraulic drop due to injection of a 2-dimensional jet into a sub-critical flow has the potentialities for utilization as a flow measurement device in small channels. Knowing injected flow Q_j , for creating a super-critical flow down stream of the jet, y_1 the sub-critical depth can be measured and thereby F_j can be calculated. Then from the plot of Q_r vs. F_j , Q_r can be found out to give the value of Q_1 . A possible method of application is given in Appendix - E.

4.5 Conclusion

As a result of an exploratory study on the interaction of a jet with a sub-critical open channel

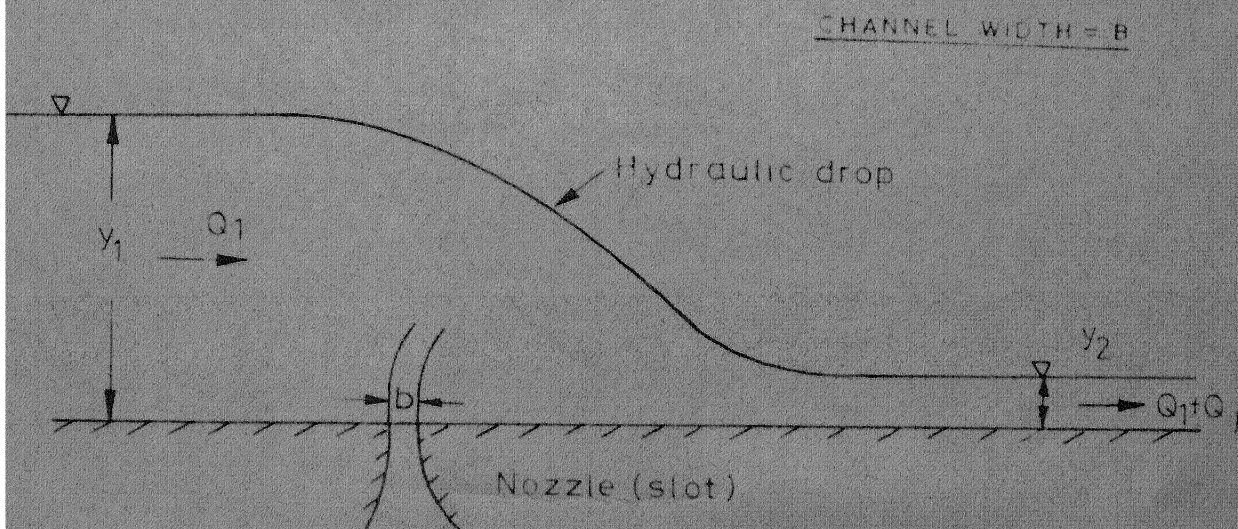


FIG. 4.1 DEFINITION SKETCH

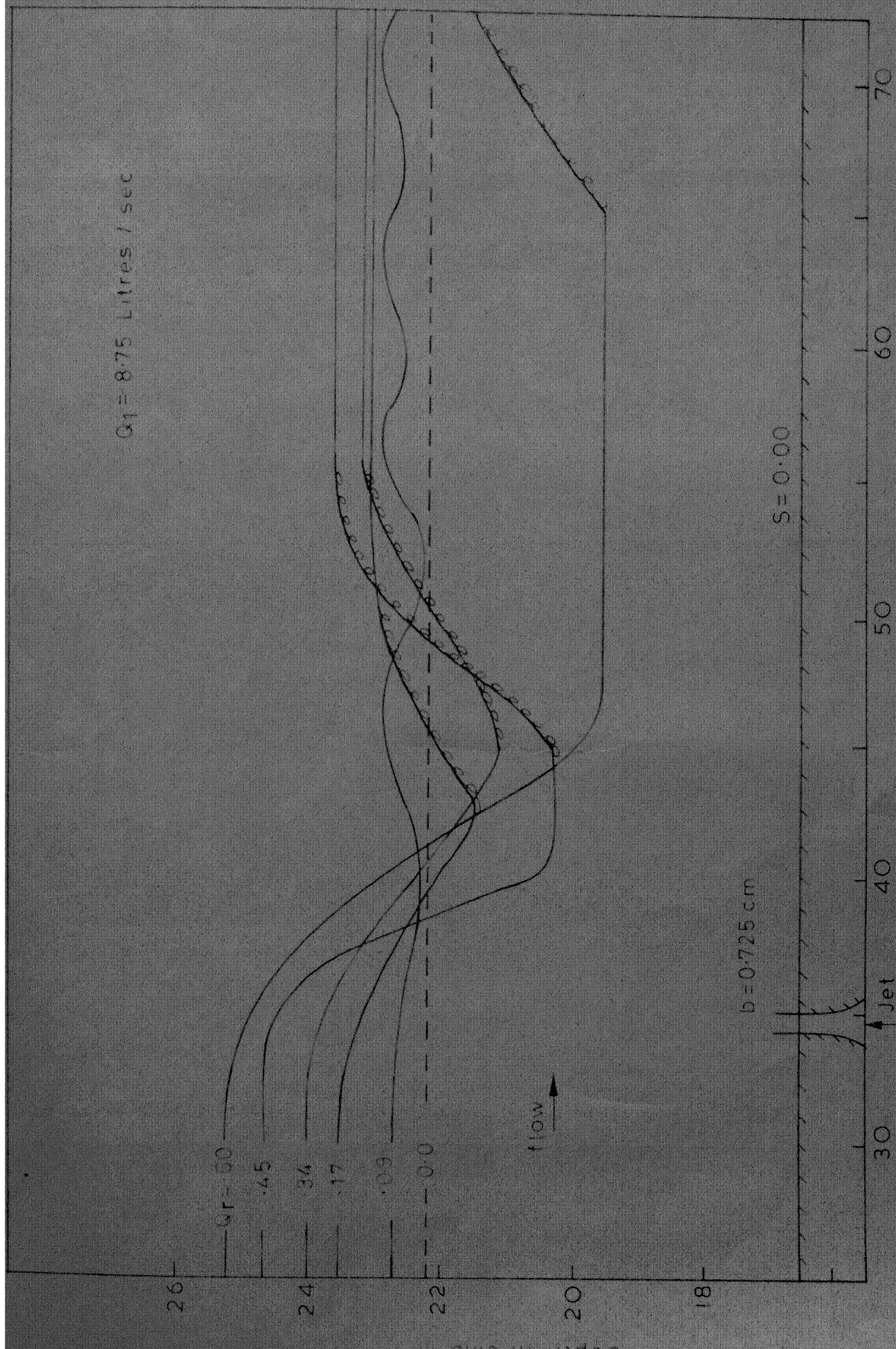


FIG. 4.2 TYPICAL WATER SURFACE PROFILES FOR DIFFERENT DISCHARGE RATIOS

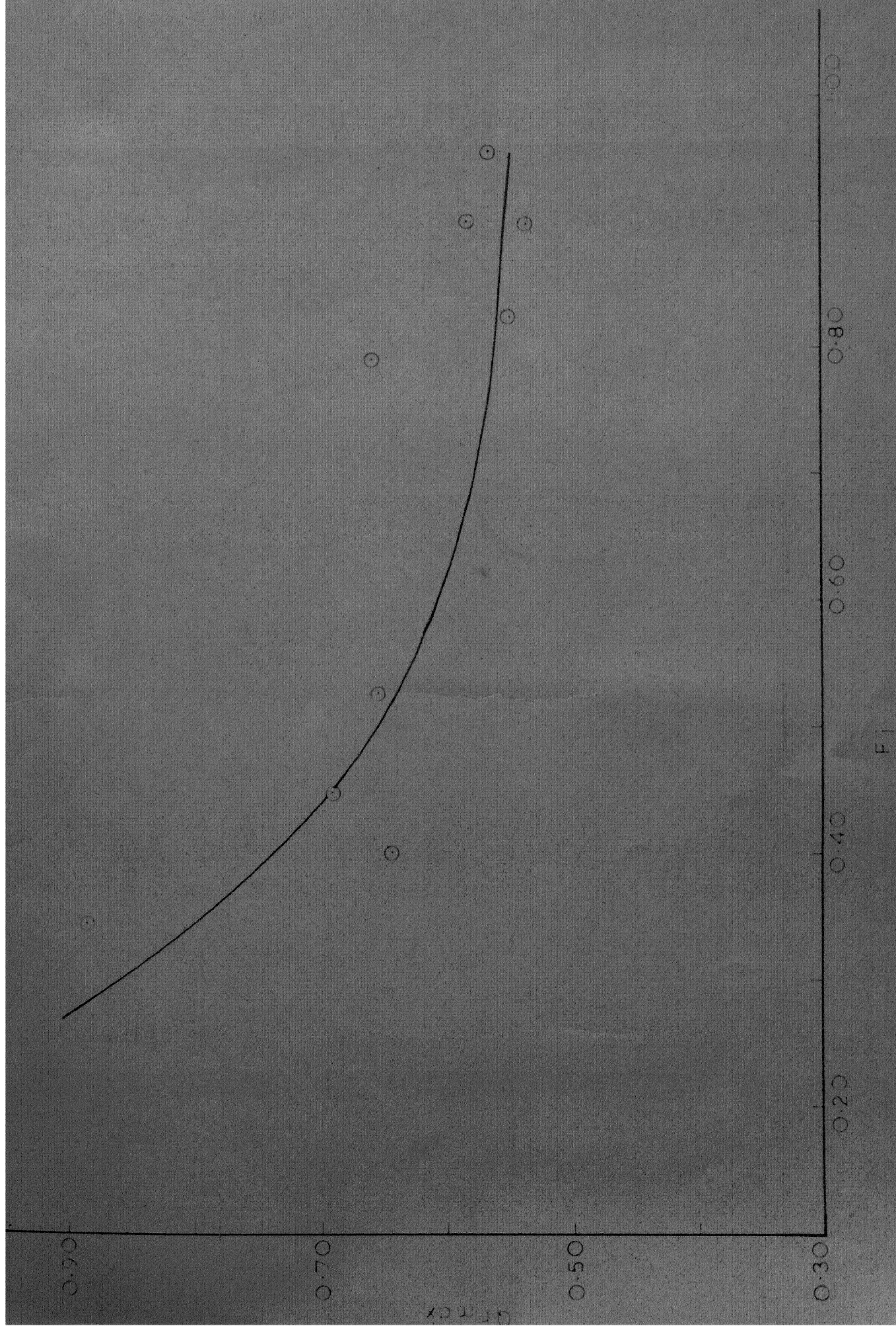
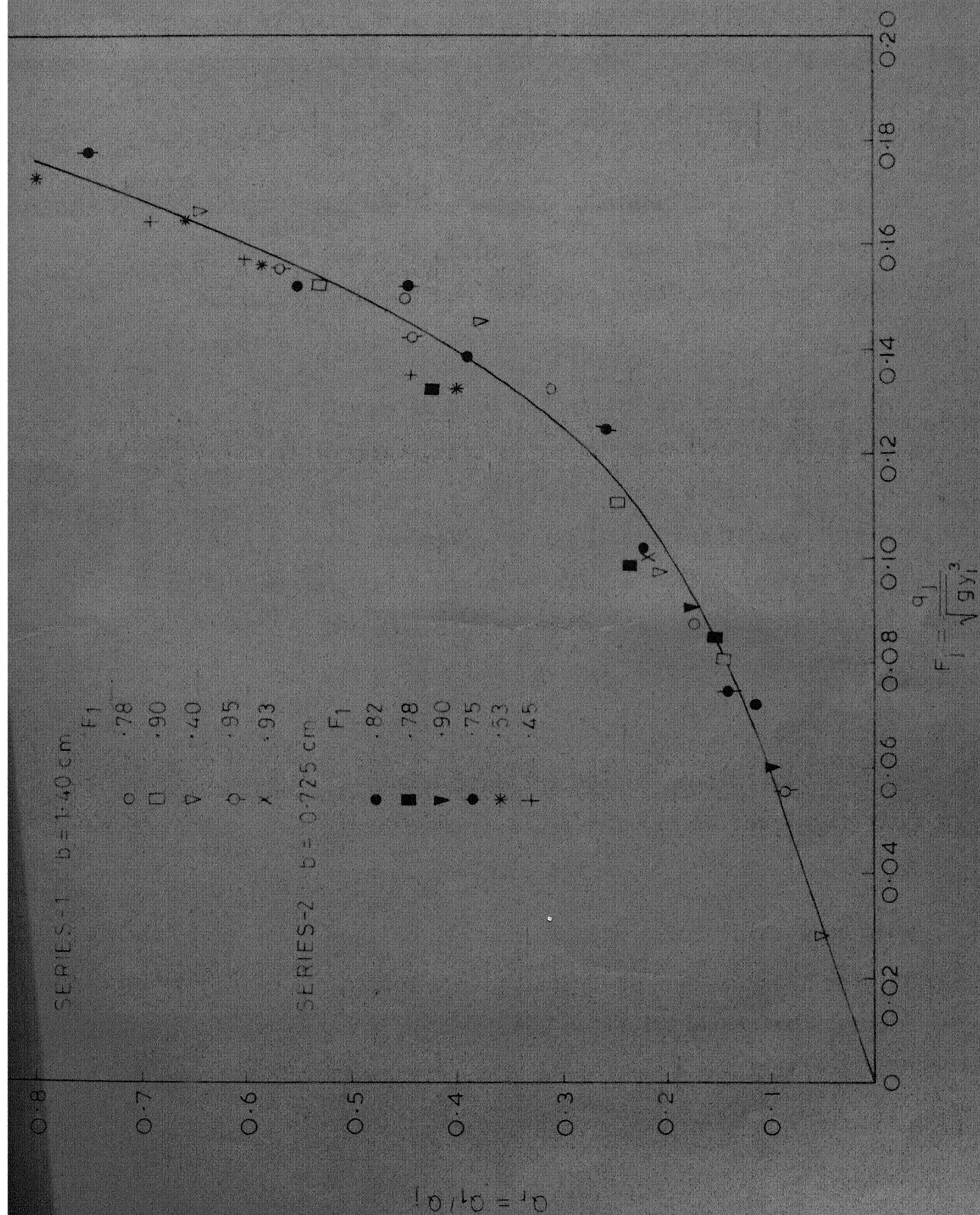


FIG. 4.3 PLOT OF INITIAL FROUDE NUMBER VS. MAXIMUM DISCHARGE RATIO

FIG. 4.4 VARIATION OF Q_r WITH F_j

CHAPTER V

CONCLUSIONS AND RECOMMENDATIONS

The various conclusions arrived at as a result of this study are given in the respective chapters in detail. However, the important conclusions are summarised here:

1. Change in flow situations in the interacting critical region for super-critical flow interacting with vertical jet is dependent only on the discharge ratio Q_r and the Froude Number F_1 of the horizontal flow as shown in Fig. 3.17. The classification of flow as in Chapter III are simple and helpful in the study of the problem
2. In type A-jump the sequent depth and other characteristics are related to the Froude Number. This is not much different from a classical jump.
3. Type-B jump has sequent depth ratio less than that of a classical jump. The energy dissipation in B jump is same as in the classical jump. This appears to have high potentials of field application.

4. In the sub-critical interaction with a vertical jet, when down stream of interaction zone is super-critical, Q_r is uniquely related to the Froude Number F_1 . Interaction of such sub-critical flow and vertical jet could be used as a flow measuring device as explained in Appendix - E.

Recommendations for further research work are

1. There is a need to study the interaction of a super-critical flow and sub-critical flow with inclined jets. The sub-critical flow interacting with a vertical jet for lower initial Froude Number will be of help in the measuring device suggested in Appendix - E.
2. Further detailed studies on B-jumps are needed.
3. B^+ jumps have to be studied to develop water baffle type energy dissipators.
4. C and C^+ jumps need study.

REFERENCES

- 1.. Chow, Ven Te : " Open Channel Hydraulics", McGraw Hill, N.Y., 1959.
- 2.. Rajaratnam, N. : "Hydraulic Jump", Advances in Hydros- science, Vol.4, Academic Press.N.Y., 1967.
3. Faktorovitch, M.E. : "Energy dissipation in the process of interaction of iminging flows!", Proc. of International national Association for Hydraulic Research, Vol.I, Eleventh Congress Leningrad, 1965.

APPENDIXES

APPENDIX - A

EXPERIMENTAL DATA FOR SUPER-CRITICAL FLOW INTERACTING WITH VERTICAL JET

S.No.	b/y_1	F_1	Q_{ra}	Q_{rc}	Q_{rd}
1	2	3	4	5	6
1	1.148	4.213	*	0.308	0.453
2	0.383	2.061	*	0.139	0.208
3	0.383	2.921	*	0.166	0.237
4	0.383	3.488	*	0.223	0.329
5	0.383	1.962	*	0.132	0.178
6	0.383	2.447	*	0.194	0.236
7	0.383	3.044	*	0.212	0.256
8	0.383	3.556	*	0.191	0.324
9	0.287	2.191	*	0.141	0.174
10	0.287	2.643	*	0.140	0.210
11	0.287	3.145	*	0.229	0.256
12	0.287	3.478	*	0.161	0.250
13	0.148	2.128	*	0.105	0.139
14	0.148	2.476	*	0.129	0.180
15	0.590	3.334	*	0.173	0.312
16	0.197	2.005	*	0.117	0.155
17	0.197	2.614	*	0.136	0.222
18	0.295	2.746	*	0.218	0.276
19	0.295	3.375	*	0.155	0.275
20	0.295	4.025	*	0.202	0.298

* No Separation

1	2	3	4	5	6
21	1.418	9.653	0.261	0.533	0.722
22	1.418	8.127	0.271	0.486	0.618
23	1.418	10.604	0.184	0.678	0.827
24	1.418	12.432	0.246	0.775	0.919
25	1.418	13.682	0.271	0.964	1.043
26	0.574	5.916	0.260	0.427	0.487
27	0.574	6.150	0.257	0.455	0.545
28	0.574	6.207	0.251	0.445	0.583
29	0.574	6.388	0.218	0.486	0.584
30	0.574	6.630	0.285	0.549	0.573
31	0.574	5.250	0.285	0.393	0.556
32	0.574	7.557	0.245	0.467	0.567
33	0.574	7.924	0.259	0.356	0.567
34	0.574	5.322	0.255	0.405	0.422
35	0.574	5.823	0.258	0.445	0.463
36	0.574	5.011	0.265	0.401	0.491
37	0.574	5.730	0.196	0.356	0.494
38	0.574	6.436	0.328	0.468	0.449
39	0.574	6.973	0.209	0.509	0.546
40	1.148	6.642	0.199	0.437	0.573

1	2	3	4	5	6
41	1.148	21.201	0.262	0.470	0.543
42	1.148	23.194	0.241	0.403	0.472
43	0.383	4.236	0.172	0.289	0.450
44	0.383	5.184	0.213	0.326	0.432
45	0.383	5.503	0.194	0.426	0.474
56	0.383	6.190	0.183	0.415	0.498
47	0.383	5.300	0.232	0.356	0.437
48	0.383	5.805	0.212	0.267	0.417
49	0.383	6.505	0.174	0.355	0.400
50	0.287	3.845	0.237	0.302	0.396
51	0.287	4.487	0.191	0.312	0.389
52	0.287	4.799	0.228	0.341	0.434
53	0.590	11.684	0.282	0.736	0.884
54	0.590	7.886	0.265	0.574	0.690
55	0.590	9.332	0.284	0.640	0.745
56	0.590	10.618	0.266	0.692	0.779
57	0.590	6.774	0.346	0.554	0.627
58	0.590	11.870	0.279	0.810	0.889
59	0.197	4.220	0.217	0.288	0.469
60	0.197	3.667	0.160	0.220	0.280

1	2	3	4	5	6
61	0.197	4.713	0.194	0.283	0.343
62	0.197	5.009	0.197	0.303	0.395
63	0.197	5.485	0.201	0.288	0.398
64	0.197	6.612	0.161	0.350	0.451
65	0.295	4.691	0.241	0.343	0.424
66	0.295	5.384	0.229	0.379	0.738
67	0.295	5.494	0.172	0.392	0.506

APPENDIX - B

EXPERIMENTAL DATA FOR TYPE - B JUMP

Sl. No.	Gate Opening	Jet Thick- ness	Q_1 Lit/Sec.	Q_2 Lit/Sec.	Y_{2B} cm	Y_{hB} cm	L_e cm
1	2	3	4	5	6	7	8
1	6.00	1.40	49.25	57.50	18.50	23.20	*
2	6.00	1.40	61.00	65.35	26.30	*	*
3	8.00	1.40	58.25	72.00	22.60	*	*
4	8.00	1.40	68.00	80.40	22.00	*	*
5	2.00	1.40	15.40	19.55	11.70	*	*
6	4.00	1.40	26.04	34.04	14.40	*	*
7	4.00	1.40	29.80	40.00	17.00	*	*
8	4.00	1.40	33.50	42.18	20.20	*	*
9	4.00	1.40	37.87	56.72	21.00	*	*
10	4.00	1.40	40.38	51.06	23.80	*	*
11	4.00	1.40	44.39	54.89	21.60	*	*
12	4.00	0.725	24.40	30.90	14.45	15.05	35.00
13	4.00	0.725	30.00	37.22	17.00	20.23	51.00
14	4.00	0.725	36.75	44.30	20.79	28.45	62.00
15	4.00	0.725	44.55	55.00	27.80	36.00	70.00

*Not recorded

Continued..

APPENDIX - B (Continued)

1	2	3	4	5	6	7	8
16	6.00	0.725	43.00	53.50	20.06	24.00	45.00
17	6.00	0.725	47.30	56.60	21.90	26.31	53.00
18	6.00	0.725	56.60	61.40	25.48	33.73	64.00
19	2.00	0.725	11.60	14.90	8.40	9.52	20.00
20	2.00	0.725	14.90	18.45	11.97	13.00	31.00
21	2.00	0.725	19.05	25.00	15.52	21.00	36.00
22	2.00	0.725	22.80	28.90	18.44	23.29	49.00

$y_1 = 0.6$ (Gate opening)

APPENDIX - C

DATA FOR TYPE B JUMPS
(Computed Parameters)

S.No.	F_1	y_{2B}/y_1	y_{hB}/y_1	Le/y_1	E_{IR}
1	5.18	5.05	6.35		0.517
2	6.15	7.20	*	*	0.596
3	3.84	4.64	*	*	0.334
4	4.49	4.50	*	*	0.479
5	8.13	9.60	*	*	0.626
6	4.96	5.90	*	*	0.407
7	5.73	6.96	*	*	0.466
8	6.40	8.30	*	*	0.493
9	7.07	8.20	*	*	0.016
10	7.63	9.75	*	*	0.597
11	8.15	9.85	*	*	0.689
12	4.50	5.93	6.15	14.35	0.410
13	5.52	6.96	8.30	20.90	0.516
14	6.75	8.40	11.65	25.40	0.596
15	8.08	11.40	14.75	28.70	0.641
16	4.32	5.50	6.55	12.30	0.471
17	4.75	6.00	7.17	14.50	0.478
18	5.66	6.96	9.20	17.50	0.548

Continued..

*Not recorded

APPENDIX - C (Continued)

S.No.	F_1	y_{2B}/y_1	y_{hB}/y_1	L_e/y_1	E_{IR}
19	6.03	6.90	7.80	16.40	0.538
20	7.70	9.80	10.65	25.40	0.613
21	9.90	12.72	17.20	29.60	0.688
22	11.85	15.10	19.10	40.20	0.744

APPENDIX — D

DATA FOR SUB-CRITICAL FLOW INTERACTING
WITH THE VERTICAL JET

Sl. No.	b cm.	Y_1 cm.	Q_1 Lit/Sec	Q_1+Q_j Lit/Sec	Q_j Lit/Sec	$Q_r = \frac{Q_j}{Q_1}$	F_j
1	2	3	4	5	6	7	8
1	1.40	4.90	12.18*	-	-	-	-
2	1.40	6.60	"	14.27	2.09	0.172	0.086
3	1.40	7.35	"	15.92	3.74	0.307	0.132
4	1.40	8.74	"	17.68	5.50	0.450	0.149
5	1.40	7.13	18.33*	-	-	-	-
6	1.40	8.50	"	19.29	0.96	0.052	0.027
7	1.40	9.20	"	22.17	3.84	0.210	0.096
8	1.40	10.35	"	25.25	6.92	0.377	0.145
9	1.40	11.42	"	27.12	8.79	0.480	0.159
10	1.40	13.64	"	30.23	11.90	0.695	0.165
11	1.40	3.27	5.68*	-	-	-	-
12	1.40	4.90	"	7.94	2.26	0.396	0.145
13	1.40	7.20	24.60*	-	-	-	-
14	1.40	10.00	"	28.23	3.63	0.148	0.081
15	1.40	11.30	"	30.63	6.03	0.245	0.111
16	1.40	16.00	"	38.52	13.92	0.535	0.152

Continued..

1	2	3	4	5	6	7	8
17	1.40	8.11	31.43*	-	-	-	-
18	1.40	10.70	"	34.18	2.75	0.087	0.055
19	1.40	16.84	"	45.34	13.91	0.442	0.142
20	1.40	18.84	"	48.97	17.34	0.566	0.154
21	1.40	2.80	6.20*	-	-	-	-
22	1.40	4.49	"	7.57	1.37	0.220	0.101
23	1.40	5.94	"	10.38	4.18	0.656	0.198
24	0.725	4.72	12.08*	-	-	-	-
25	0.725	6.14	"	13.64	1.56	0.129	0.072
26	0.725	6.75	"	14.77	2.69	0.222	0.108
27	0.725	8.20	"	16.72	4.64	0.384	0.138
28	0.725	9.85	"	18.75	6.67	0.550	0.151
29	0.725	8.66	28.95*	-	-	-	-
30	0.725	10.97	"	33.36	4.41	0.152	0.085
31	0.725	13.30	"	35.75	6.80	0.235	0.099
32	0.725	16.18	"	41.16	12.21	0.422	0.132

Continued..

1	2	3	4	5	6	7	8
33	0.725	3.66	7.51*	-	-	-	-
34	0.725	4.62	"	8.56	1.05	0.139	0.074
35	0.725	5.00	"	9.45	1.94	0.258	0.124
36	0.725	6.23	"	10.85	3.34	0.445	0.151
37	0.725	7.92	"	13.15	5.64	0.750	0.177
38	0.725	5.89	18.33*	-	-	-	-
39	0.725	8.63	"	21.60	3.27	0.177	0.090
40	0.725	7.86	"	20.22	1.89	0.103	0.060
41	0.725	12.80	"	27.22	8.89	0.485	0.136
42	0.725	5.72	8.75*	-	-	-	-
43	0.725	7.56	"	12.75	4.00	0.445	0.135
44	0.725	8.15	"	14.00	5.25	0.600	0.158
45	0.725	8.73	"	14.80	7.05	0.690	0.164
46	0.725	6.72	13.10*	-	-	-	-
47	0.725	9.18	"	18.35	5.25	0.400	0.132
48	0.725	10.50	"	20.75	7.65	0.585	0.157
49	0.725	11.00	"	21.64	8.54	0.655	0.165

* Initial values. F_i = Initial Froude number corresponds to these values

APPENDIX-E

A POSSIBLE APPLICATION OF SUB-CRITICAL
FLOW JET INTERACTION

The hydraulic drop formation due to the injection of an upward issuing jet at the bottom of a free surface sub-critical open-channel flow can be utilised as a discharge measuring device.

A diagram of the set-up, which can be used to measure the discharge in small channel is given in Fig.E-1. Essentially this unit consists of (a) pumping set (b) Flexible pipe (c) a jet assembly and (d) a mattress for downstream protection from the super-critical flow created by the jet.

Procedure: The discharge for the jet is taken from down stream side of the nozzle. The jet discharge Q_j which will produce a drop and a super critical flow down stream of the jet, is pumped through a ~~nozzle~~ *nozzle*. The resulting upstream depth y_1 is measured. Knowing the depth y_1 and jet discharge Q_j , the parameter F_j defined in chapter IV can be calculated. For this F_j the value of discharge ratio Q_r

E-2

can be obtained from Fig. 4.4. Once Q_r is known, then Q_1 the discharge in the channel can be found out.

An alternative method of taking discharge from the downstream of the jet is to take the discharge Q_j from upstream side of the jet. The discharge in the channel will be the sum of Q_1 and Q_j . However care must be taken, that there will not be any disturbances in the vicinity of the jet.

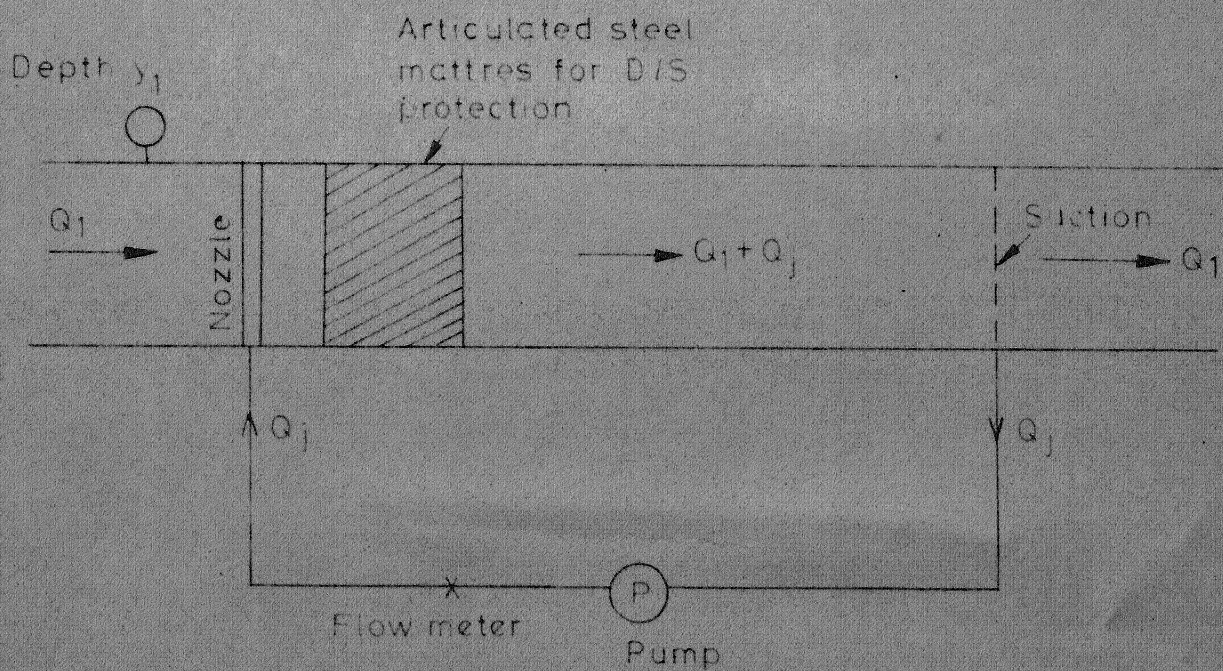


FIG. E-1 SCHEMATIC DIAGRAM OF A POSSIBLE APPLICATION